Cellular/Molecular

Redistribution of $GABA_{B(1)}$ Protein and Atypical $GABA_B$ Responses in $GABA_{B(2)}$-Deficient Mice

Martin Gassmann,[1]* Hamdy Shaban,[2,3]* Réjan Vigot,[1]* Gilles Sansig,[4] Corinne Haller,[1] Samuel Barbieri,[1] Yann Humeau,[2,3,5] Valérie Schuler,[4] Matthias Müller,[4] Bernd Kinzel,[4] Klaus Klebs,[4] Markus Schmutz,[4] Wolfgang Froestl,[4] Jakob Heid,[4] Peter H. Kelly,[4] Clive Gentry,[6] Anne-Lise Jaton,[4] Herman Van der Putten,[4] Cédric Mombereau,[4] Lucas Lecourtier,[4] Johannes Mosbacher,[4] John F. Cryan,[4] Jean-Marc Fritschy,[7] Andreas Lüthi,[2,3] Klemens Kaupmann,[4] and Bernhard Bettler[1]

[1]Pharmazentrum, Department of Clinical-Biological Sciences, University of Basel, CH-4056 Basel, Switzerland, [2]Friedrich Miescher Institute, CH-4058 Basel, Switzerland, [3]Biozentrum, University of Basel, CH-4056 Basel, Switzerland, [4]Novartis Institutes for Biomedical Research, Novartis Pharma AG, CH-4002 Basel, Switzerland, [5]Centre National de la Recherche Scientifique, Unité Propre de Recherche 2356, F-67084 Strasbourg, France, [6]Novartis Institute for Medical Sciences, London WC1E 6B9, United Kingdom, and [7]Institute of Pharmacology and Toxicology, University of Zürich, CH-8057 Zürich, Switzerland

$GABA_B$ receptors mediate slow synaptic inhibition in the nervous system. In transfected cells, functional $GABA_B$ receptors are usually only observed after coexpression of $GABA_{B(1)}$ and $GABA_{B(2)}$ subunits, which established the concept of heteromerization for G-protein-coupled receptors. In the heteromeric receptor, $GABA_{B(1)}$ is responsible for binding of GABA, whereas $GABA_{B(2)}$ is necessary for surface trafficking and G-protein coupling. Consistent with these *in vitro* observations, the $GABA_{B(1)}$ subunit is also essential for all $GABA_B$ signaling *in vivo*. Mice lacking the $GABA_{B(1)}$ subunit do not exhibit detectable electrophysiological, biochemical, or behavioral responses to $GABA_B$ agonists. However, $GABA_{B(1)}$ exhibits a broader cellular expression pattern than $GABA_{B(2)}$, suggesting that $GABA_{B(1)}$ could be functional in the absence of $GABA_{B(2)}$. We now generated $GABA_{B(2)}$-deficient mice to analyze whether $GABA_{B(1)}$ has the potential to signal without $GABA_{B(2)}$ in neurons. We show that $GABA_{B(2)}{}^{-/-}$ mice suffer from spontaneous seizures, hyperalgesia, hyperlocomotor activity, and severe memory impairment, analogous to $GABA_{B(1)}{}^{-/-}$ mice. This clearly demonstrates that the lack of heteromeric $GABA_{B(1,2)}$ receptors underlies these phenotypes. To our surprise and in contrast to $GABA_{B(1)}{}^{-/-}$ mice, we still detect atypical electrophysiological $GABA_B$ responses in hippocampal slices of $GABA_{B(2)}{}^{-/-}$ mice. Furthermore, in the absence of $GABA_{B(2)}$, the $GABA_{B(1)}$ protein relocates from distal neuronal sites to the soma and proximal dendrites. Our data suggest that association of $GABA_{B(2)}$ with $GABA_{B(1)}$ is essential for receptor localization in distal processes but is not absolutely necessary for signaling. It is therefore possible that functional $GABA_B$ receptors exist in neurons that naturally lack $GABA_{B(2)}$ subunits.

Key words: **GABA; GPCR; G-protein; heterodimerization; metabotropic; trafficking**

Introduction

GABA, the predominant inhibitory neurotransmitter in the mammalian nervous system, signals through ionotropic $GABA_A$ and metabotropic $GABA_B$ receptors. $GABA_B$ receptors are coupled to G-proteins and modulate synaptic transmission by activating postsynaptic inwardly rectifying Kir3-type K^+ channels and by controlling neurotransmitter release (Bowery et al., 2002; Calver et al., 2002; Bettler et al., 2004).

Molecular studies on $GABA_B$ receptors provide compelling evidence for heteromerization among G-protein-coupled receptors (GPCRs) (Marshall et al., 1999; Möhler et al., 2001). Most experiments with cloned $GABA_{B(1)}$ and $GABA_{B(2)}$ subunits expressed in heterologous cells and sympathetic neurons (Filippov et al., 2000) indicate that individual subunits are functionally inert unless they are coexpressed. $GABA_B$ receptors therefore appear different from other heterodimeric GPCRs in which individual subunits are functional when expressed alone (Bouvier, 2001). In the $GABA_B$ heteromer, the $GABA_{B(1)}$ subunit binds GABA and all competitive $GABA_B$ ligands (Kaupmann et al., 1998), whereas the $GABA_{B(2)}$ subunit is responsible for escorting $GABA_{B(1)}$ to the cell surface and for activating the G-protein (Margeta-Mitrovic et al., 2000, 2001b; Calver et al., 2001; Galvez et al., 2001; Pagano et al., 2001; Robbins et al., 2001). Two $GABA_{B(1)}$ isoforms, $GABA_{B(1a)}$ and $GABA_{B(1b)}$, arise by differential promoter usage (Kaupmann et al., 1997; Bettler et al., 2004). Thus far, the data support the existence of two predominant, yet pharmacologically indistinguishable, $GABA_B$ receptors in the nervous system, the heteromeric $GABA_{B(1a,2)}$ and $GABA_{B(1b,2)}$ receptors.

Received Oct. 31, 2003; revised April 27, 2004; accepted April 27, 2004.

This work was supported by Swiss Science Foundation Grant 3100-067100.01 (B.B.). We thank Rita Meyerhofer, Hugo Buerki, C. Sidler, and F. Parpan for technical support, K. Sauter for genotyping, and D. Benke, C. Lüscher, and all members of the Bettler laboratory for helpful discussions.

*M.G., H.S., and R.V. contributed equally to this work.

Correspondence should be addressed to either of the following: Bernhard Bettler, Biozentrum/Pharmazentrum, University of Basel, Klingelbergstrasse 50, CH-4056 Basel, Switzerland, E-mail: bernhard.bettler@unibas.ch; or Klemens Kaupmann, Novartis Institutes for Biomedical Research, Novartis Pharma AG, CH-4002 Basel, Switzerland. E-mail: klemens.kaupmann@pharma.novartis.com.

DOI:10.1523/JNEUROSCI.5635-03.2004

 0270-6474/04/246086-12$15.00/0

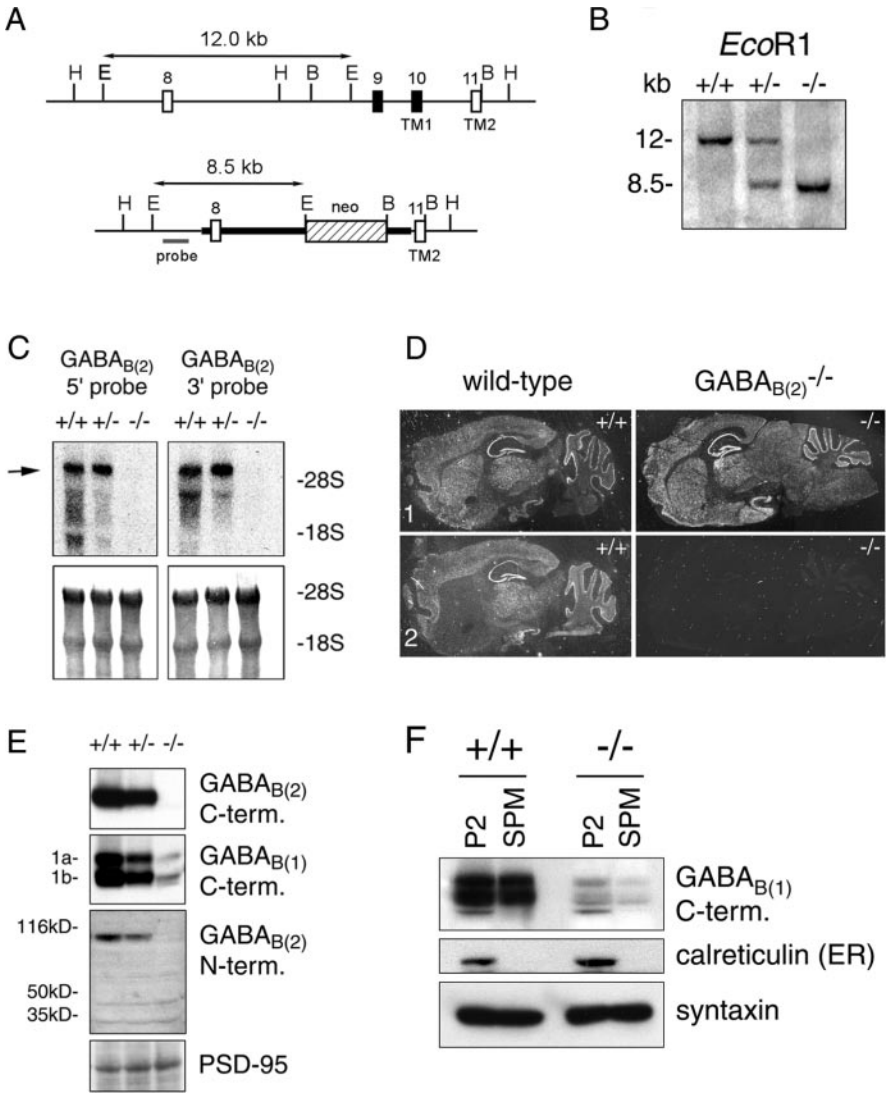

Figure 1. Characterization of $GABA_{B(2)}^{-/-}$ mice. *A*, Top, $GABA_{B(2)}$ locus encompassing exons 8–11, encoding part of the N-terminal and the transmembrane (TM) domains 1 and 2. Bottom, $GABA_{B(2)}$ allele after homologous recombination with a targeting construct containing a neomycin resistance cassette (neo) flanked by 4.5 and 1.8 kb of genomic DNA (bold lines). Exons 9 and 10 (3.5 kb, black boxes) are deleted. The Southern blot probe used in *B* is indicated. H, *Hind*III; E, *Eco*RI; B, *Bam*HI. *B*, Southern blot analysis of *Eco*RI cut genomic DNA from wild-type (+/+), $GABA_{B(2)}^{+/-}$ (+/−), and $GABA_{B(2)}^{-/-}$ (−/−) mice. *C*, Top, Northern blot analysis of total brain RNA hybridized with $GABA_{B(2)}$ cDNA probes upstream (5′ probe) and downstream of the deletion (3′ probe). The probes hybridize to a band just above the 28 S ribosomal RNA (arrow) in wild-type and $GABA_{B(2)}^{+/-}$, but not in $GABA_{B(2)}^{-/-}$, mice. Bottom, Blots from top panels stained with methylene blue, demonstrating equal loading of RNA. Ribosomal RNA bands (18 and 28 S) are labeled. *D*, *In situ* hybridization analysis of $GABA_{B(1)}$ (1, top) and $GABA_{B(2)}$ (2, bottom) transcripts of sagittal sections from adult wild-type and $GABA_{B(2)}^{-/-}$ brains. *E*, Immunoblot analysis of brain extracts from adult mice using antibodies directed against C-terminal and N-terminal epitopes of $GABA_{B(2)}$ and $GABA_{B(1)}$. Antibodies to PSD-95 control for equal loading. $GABA_{B(1a)}$ (1a) and $GABA_{B(1b)}$ (1b) proteins are indicated. *F*, Immunoblot analysis demonstrating the presence of $GABA_{B(1)}$ protein in synaptic plasma membranes (SPM) purified from the P2 pellet (P2) of brain extracts of wild-type and $GABA_{B(2)}^{-/-}$ mice. Antibodies to calreticulin show that the synaptic plasma membrane fraction is free of ER proteins. Equal loading of samples was controlled with anti-syntaxin antibodies. To detect putative truncated $GABA_{B(2)}$ proteins, we used 15% SDS-PAGE and N-terminal $GABA_{B(2)}$ antibodies. In all other immunoblot experiments, we used 10% SDS-PAGE.

$GABA_{B(1)}^{-/-}$ mice do not exhibit detectable $GABA_B$ responses in a variety of experimental paradigms, demonstrating that $GABA_{B(1)}$ is not only essential for $GABA_B$ signaling *in vitro* but also *in vivo* (Prosser et al., 2001; Schuler et al., 2001; Quéva et al., 2003). However, no *in vivo* experiment addressed whether $GABA_{B(1)}$ can assemble functional $GABA_B$ receptors by itself or in association with a protein other than $GABA_{B(2)}$. In support of a separate role, $GABA_{B(1)}$ exhibits a more widespread cellular distribution than does $GABA_{B(2)}$ (Kaupmann et al., 1998; Clark et al., 2000; Ng and Yung, 2001; Burman et al., 2003; Kim et al., 2003; Kulik et al., 2003; Li et al., 2003). Furthermore, at odds with a strict requirement of $GABA_{B(2)}$ for plasma membrane delivery, $GABA_{B(1)}$ was originally cloned by surface expression in mammalian cells (Kaupmann et al., 1997). Additionally, $GABA_{B(1)}$ occasionally yields electrophysiological or biochemical responses when transfected alone into heterologous cells (Kaupmann et al., 1997, 1998). It is therefore conceivable that $GABA_{B(1)}$ is functional either alone or in combination with an unknown protein. However, it remains unclear whether sporadic endogenous expression of $GABA_{B(2)}$ in heterologous cells is responsible for the surface expression and the responses that were seen when $GABA_{B(1)}$ was transfected alone.

To clarify whether $GABA_{B(1)}$ can participate in functional $GABA_B$ receptors in the absence of $GABA_{B(2)}$, we generated mice with a loss-of-function mutation in the $GABA_{B(2)}$ gene. Our results show that all well known $GABA_B$ responses relate to heteromeric $GABA_{B(1,2)}$ receptors. Surprisingly, the experiments also reveal atypical $GABA_B$ responses in hippocampal slices of $GABA_{B(2)}$-deficient mice, indicating that $GABA_{B(1)}$ assemblies could be operational in neurons that naturally lack $GABA_{B(2)}$.

Materials and Methods

Generation and analysis of $GABA_{B(2)}^{-/-}$ mice. $GABA_{B(2)}^{-/-}$ mice were generated in the BALB/c inbred strain using a newly established BALB/c embryonic stem (ES) cell line. A targeting construct was designed containing a neomycin resistance cassette (pRay-2; GenBank accession number U63120) flanked by 4.5 and 1.8 kb of genomic $GABA_{B(2)}$ DNA that was amplified from a C57BL/6 bacterial artificial chromosome. Homologous recombination was confirmed by Southern blot analysis (Fig. 1*A*,*B*). Selected ES cell clones were microinjected into C57BL/6 blastocysts. Chimeric males were crossed with BALB/c females, resulting in an F1 generation of inbred BALB/c $GABA_{B(2)}^{+/-}$ mice. $GABA_{B(2)}^{+/-}$ mice were viable and fertile and allowed the generation of $GABA_{B(2)}^{-/-}$ mice in the F2 generation. The probes used in Northern blot analysis (Fig. 1*C*) hybridize to exons 4–8 and exons 11–15 upstream (5′ probe) and downstream (3′ probe) of the deletion, respectively (Martin et al., 2001). For *in situ* hybridization (Fig. 1*D*), antisense oligonucleotides corresponding to nucleotides 2039–79 and 1810–54 of the rat $GABA_{B(1a)}$ (GenBank accession number Y10369) and $GABA_{B(2)}$ (GenBank accession number AJ011318) cDNAs, respectively, were used. The probes were radiolabeled with [^{35}S]dATP (NEG0345H; NEN, Boston, MA) using terminal deoxynucleotidyl transferase (Promega, Madison, WI). For immunoblot analysis (Fig. 1*E*,*F*), polyclonal antibodies directed against the C terminus of $GABA_{B(2)}$ (AB5394; Chemicon, Temecula, CA), the C terminus of $GABA_{B(1)}$ (antibody

174.1) (Malitschek et al., 1998), the N terminus of $GABA_{B(2)}$ (antibody N22) (Kaupmann et al., 1998), and mouse calreticulin (ab4; Abcam, Cambridge, UK) were used. Monoclonal antibodies were used to detect PSD-95 (postsynaptic density protein-95) (MAB1598, Chemicon) and syntaxin (Sigma, St. Louis, MO). Blots were exposed to HRP-conjugated secondary antibodies [NA9340 (Amersham Biosciences, Little Chalfont, UK); A5545 and A0168 (Fluka, Buchs, Switzerland)] and developed using the ECL chemiluminescent detection system (RPN2016; Amersham Biosciences). Brain membrane preparations, ligand binding assays, and receptor autoradiography were performed as described previously (Olpe et al., 1990; Kaupmann et al., 1997). Synaptic plasma membranes were isolated from the P2 pellets of brain lysates by combined flotation–sedimentation density-gradient centrifugation (Jones and Matus, 1974). [^{3}H]CGP62349 (80 Ci/mmol), [^{3}H]CGP54626 (40 Ci/mmol), [^{125}I]CGP71872 (2000 Ci/mmol), and [^{125}I]CGP64213 (2000 Ci/mmol) were purchased from ANAWA (Wangen, Switzerland). [^{35}S]GTPγS (1000 Ci/mmol) was obtained from Amersham Biosciences. Nonradioactive $GABA_B$ receptor ligands were from Novartis (Basel, Switzerland). [^{35}S]GTPγS binding was performed with 20 μg of membrane protein, 0.2 nM [^{35}S]GTPγS, and test compounds in 96-well Packard (Meridian, CT) Pico-Plates as described previously (Urwyler et al., 2001).

Immunohistochemistry. Immunoperoxidase staining was performed in brain sections of adult mice using guinea pig antisera against $GABA_{B(2)}$ (1:5000; AB5394; Chemicon) and $GABA_{B(1)}$ (1:3000; AB1531; Chemicon). Mice were deeply anesthetized with Nembutal (50 mg/kg) and perfused through the ascending aorta with 4% paraformaldehyde in 0.15 M phosphate buffer. Brains were postfixed for 3 hr, processed for antigen retrieval using microwave irradiation (Fritschy et al., 1998), cryoprotected in sucrose, and cut at 40 μm with a sliding microtome. The immunoperoxidase staining was performed using diaminobenzidine as chromogen (Fritschy et al., 1999). Tissue from different genotypes was processed together to minimize variability attributable to the staining procedure. Sections were analyzed by light microscopy (Axioskop; Zeiss, Jena, Germany) and photographed with a high-resolution digital camera.

Electrophysiology. Transverse hippocampal slices (350-μm-thick) from 3- to 4-week-old mice were prepared. Slices were maintained for 45 min at 35°C in an interface chamber containing saline equilibrated with 95% O_2 and 5% CO_2 and containing the following (in mM): 124 NaCl, 2.7 KCl, 2 $CaCl_2$, 1.3 $MgCl_2$, 26 $NaHCO_3$, 1.24 NaH_2PO_4, 18 glucose, and 2.25 ascorbate. Slices were then kept for at least 45 min at room temperature before being transferred to a superfusing recording chamber. Whole-cell recordings from CA1 pyramidal cells were performed at 30–32°C using infrared videomicroscopy to visualize cells. Patch electrodes (3–5 MΩ) were filled with a solution containing the following (in mM): 140 Cs-gluconate, 10 HEPES, pH 7.25, 10 phosphocreatine, 5 QX-314-Cl, 4 Mg-ATP, and 0.3 Na-GTP (295 mOsm). For measurements of postsynaptic holding currents (at −50 mV, in 0.5 μM TTX), Cs-gluconate was replaced by equimolar K-gluconate, and QX-314 was omitted. Synaptic currents were elicited every 15 sec using a bipolar platinum–iridium electrode (diameter, 25 μm). EPSCs were measured at −70 mV in the presence of picrotoxin (100 μM). IPSCs were measured at 0 mV in the presence of kynurenic acid (2 mM). All experiments assessing presynaptic $GABA_B$ receptor function were performed in the presence of $BaCl_2$ (200 μM) to prevent the activation of postsynaptic Kir3 channels. $BaCl_2$ did not affect the EPSC or IPSC amplitudes. Current–voltage (*I–V*) relationships were assessed by ramp-command protocols (from −40 to −140 mV, 250 msec duration) before and after the application of agonists, and the agonist-induced *I–V* relationship was derived by subtraction. Data were recorded with an Axopatch 200B (Axon Instruments, Union City, CA), filtered at 2 kHz, and digitized at 10 kHz. Data were acquired and analyzed with the LTP Program (W. Anderson, University of Bristol, Bristol, UK) (Anderson and Collingridge, 2001) or with pClamp8.0 (Axon Instruments). All membrane potentials were corrected for the experimentally measured liquid junction potential of 11 mV for the internal K-gluconate solution. Slope conductance was determined between −140 mV and the reversal potential. Series resistance was monitored throughout the experiments by applying a hyperpolarizing pulse, and, if it changed >15%, the data were not included in the analysis. All values are expressed as means ± SEM. Statistical comparisons were done with paired or unpaired Student's *t* test as appropriate, at a significance level of 0.05. $GABA_B$ receptor ligands were from Novartis. Non-GABAergic drugs were from Fluka.

Electroencephalogram measurements. Electroencephalogram (EEG) measurements were performed as described previously (Schuler et al., 2001; Kaupmann et al., 2003). The behavior of the mice, which were individually housed in wooden observation cages, was monitored with a video system. EEGs were amplified using an isolated four-channel bipolar EEG amplifier (EEG-2104; Spectralab, Maharashtra, India), recorded on a thermo recorder (MTK95; Astro-Med, West Warwick, RI), and stored on disk.

Measurement of core body temperature, locomotor activity, rotarod, and memory performance. Rectal temperature was determined to the nearest 0.1°C as described previously (Schuler et al., 2001; Kaupmann et al., 2003). Statistical analysis was performed using repeated-measures ANOVA, followed by Fisher's least significant difference test when appropriate. Locomotor activity was recorded using a color video camera, surveying the open field, and analyzed using EthoVision 1.90 software (Noldus Information Technology, Wageningen, The Netherlands). To assess rotarod performance, mice were trained to stay on the rotarod (12 rpm) for 300 sec over two separate sessions the day before the experiment. During the test day, the length of time each mouse remained on the cylinder ("endurance time"; maximal score of 300 sec) was measured immediately before (time 0) and 1, 2, and 4 hr after the application of L-baclofen (12.5 mg/kg) or vehicle (0.5% methylcellulose). The dose of baclofen that shows maximal effects on rotarod performance was determined in previous studies (Schuler et al., 2001). Memory performance in the passive avoidance test was performed as described previously (Venable and Kelly, 1990; Schuler et al., 2001).

Nociceptive tests. Heat or mechanical nociceptive stimuli were used in the antinociceptive tests as described previously (Schuler et al., 2001). The hotplate (Eddy and Leimbach, 1953), tail-flick (D'Amour and Smith, 1941), and the paw-pressure tests (Randall and Selitto, 1957) are well established techniques to assess acute pain. The tail flick is a reflex response to a noxious thermal stimulus applied to the tail and is generally held to represent a spinal reflex response, whereas the hotplate response to a noxious thermal stimulus to the plantar surface of the paws is thought to involve supraspinal sites.

Results

Previous experiments showed that only $GABA_{B(1)}{}^{-/-}$ mice generated in the inbred BALB/c genetic background are viable (Prosser et al., 2001; Schuler et al., 2001; Quéva et al., 2003). We therefore ablated the *GABA*$_{B(2)}$ gene in BALB/c ES cells (Fig. 1*A*). Southern blot analysis confirms deletion of exons 9 (81 bp) and 10 (151 bp), encoding part of the N-terminal extracellular and the first transmembrane domain of $GABA_{B(2)}$ (Fig. 1*B*). BALB/c $GABA_{B(2)}{}^{-/-}$ mice are viable, occur at a Mendelian ratio, and do not express detectable $GABA_{B(2)}$ mRNA, as shown by Northern blot analysis using hybridization probes flanking the *GABA*$_{B(2)}$ gene deletion (Fig. 1*C*). This demonstrates that any truncated mRNA produced from the 5′ part of the *GABA*$_{B(2)}$ gene is highly unstable. The complete lack of $GABA_{B(2)}$ mRNA is confirmed by *in situ* hybridization (Fig. 1*D*). Hence, $GABA_{B(2)}{}^{-/-}$ mice do not express any full-length or truncated $GABA_{B(2)}$ protein, as shown by immunoblotting using antibodies directed against extreme C- or N-terminal epitopes (Fig. 1*E*). Immunoblot analysis further reveals that $GABA_{B(2)}{}^{+/-}$ mice express less $GABA_{B(2)}$ protein than wild-type mice. A densitometric analysis of *in situ* hybridizations from several brain sections reveals that $GABA_{B(1)}$ mRNA expression in $GABA_{B(2)}{}^{-/-}$ mice is not significantly changed when compared with wild-type littermates (Fig. 1*D*). However, immunoblot analysis indicates an ~50 and 90% reduction of $GABA_{B(1)}$ protein in $GABA_{B(2)}{}^{+/-}$ and $GABA_{B(2)}{}^{-/-}$ mice, re-

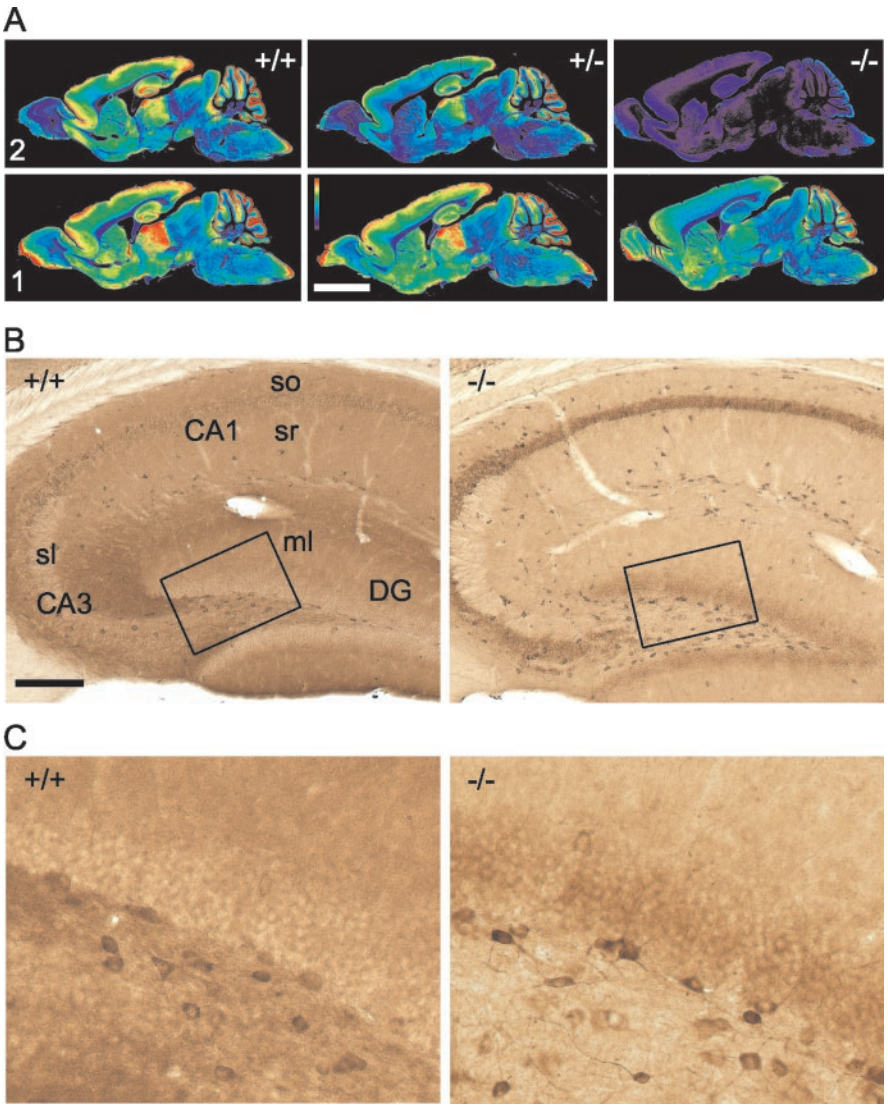

Figure 2. Alteration of $GABA_B$ receptor-IR in $GABA_{B(2)}^{-/-}$ brains. *A*, Effect of *$GABA_{B(2)}$* gene deletion on the distribution of $GABA_{B(2)}$-IR (2) and $GABA_{B(1)}$-IR (1), as visualized in color-coded parasagittal sections from adult wild-type (+/+), $GABA_{B(2)}^{+/-}$ (+/−), and $GABA_{B(2)}^{-/-}$ (−/−) mice. The color scale is indicated. The reduced expression of $GABA_{B(2)}$ in $GABA_{B(2)}^{+/-}$ mice and the complete loss of expression in $GABA_{B(2)}^{-/-}$ mice are evident throughout the brain (top). $GABA_{B(1)}$-IR is retained in $GABA_{B(2)}^{+/-}$ mice and partly reduced in $GABA_{B(2)}^{-/-}$ mice, in which it exhibits an altered cellular distribution, as seen in the hippocampus (bottom). The residual $GABA_{B(1)}$-IR in $GABA_{B(2)}^{-/-}$ mice is not caused by nonspecific binding of the secondary antibodies, which are the same for $GABA_{B(1)}$ and $GABA_{B(2)}$. The specificity of the $GABA_{B(1)}$ antiserum was also tested in $GABA_{B(1)}^{-/-}$ mice, in which no specific staining was observed (data not shown). *B*, Color photomicrographs of the hippocampal formation stained for $GABA_{B(1)}$ in adult wild-type and $GABA_{B(2)}^{-/-}$ mice. The pronounced increase of IR in the CA1–CA3 pyramidal cell layer and in the dentate gyrus granule cell layer (DG) contrasts with the strong reduction in the dendritic layers [stratum oriens (so), stratum radiatum (sr), stratum lucidum (sl), and molecular layer (ml)]. *C*, Enlargement of the framed areas in *B*. Numerous interneurons, which are primarily hidden in sections from wild-type mice because of the homogeneous staining, appear more strongly labeled in $GABA_{B(2)}^{-/-}$ mice but with a normal distribution and morphology. Scale bars: *A*, 2 mm; *B*, 200 μm.

spectively (Fig. 1*E*). This is reminiscent of the almost complete absence of $GABA_{B(2)}$ protein previously seen in $GABA_{B(1)}^{-/-}$ mice and yet again demonstrates that the two subunits cross-stabilize each other (Prosser et al., 2001; Schuler et al., 2001; Quéva et al., 2003). Despite this considerable downregulation, we clearly detect $GABA_{B(1)}$ protein in synaptic plasma membrane preparations of $GABA_{B(2)}^{-/-}$ mice (Fig. 1*F*). This indicates that *in vivo* some $GABA_{B(1)}$ protein exits the endoplasmatic reticulum (ER) in the absence of the $GABA_{B(2)}$ subunit.

Redistribution of $GABA_{B(1)}$ in $GABA_{B(2)}^{-/-}$ neurons

The regional and cellular distribution of $GABA_B$ subunits was investigated using antibodies recognizing $GABA_{B(2)}$ or the common C terminus of $GABA_{B(1a)}$ and $GABA_{B(1b)}$ (Fig. 2). A comparison of $GABA_{B(2)}$-immunoreactivity (IR) and $GABA_{B(1)}$-IR in adjacent sections of wild-type mice reveals a mostly overlapping distribution throughout the brain, with strong staining in cerebellum, thalamus, and hippocampal formation (Fig. 2*A*). In $GABA_{B(2)}^{+/-}$ mice, $GABA_{B(2)}$-IR is reduced in all brain regions, whereas $GABA_{B(1)}$-IR remains similar to wild-type mice. In $GABA_{B(2)}^{-/-}$ mice, a partial expression of $GABA_{B(1)}$-IR is still seen in most brain regions, contrasting with the complete loss of $GABA_{B(2)}$ expression. At higher magnification, $GABA_{B(1)}$-IR in $GABA_{B(2)}^{-/-}$ mice exhibits a strikingly different cellular distribution than in wild-type mice, as illustrated for the hippocampal formation (Fig. 2*B*). The homogeneous, diffuse staining of the neuropil is almost reduced to background level, whereas the cell body layers, which normally are weakly labeled in wild-type mice, now appear very prominent. In addition, some scattered hippocampal interneurons are more evident in $GABA_{B(2)}^{-/-}$ than in wild-type mice. The $GABA_{B(1)}$-IR prominently outlines the soma and the proximal dendrites of these isolated interneurons, shown at higher magnification in Figure 2*C*. Similar results were observed throughout the brain, with an apparent accumulation of $GABA_{B(1)}$-IR in the soma and proximal dendrites and a corresponding reduction of neuropil staining (data not shown). This staining was specific because no $GABA_{B(1)}$-IR was detected in brain sections from $GABA_{B(1)}^{-/-}$ mice, which were used as a control (data not shown). It is impossible to conclusively determine whether the $GABA_{B(1)}$-IR seen in $GABA_{B(2)}^{-/-}$ mice is partly associated with the plasma membrane or not. However, the strong $GABA_{B(1)}$-IR in proximal dendrites of scattered interneurons, as shown in the hippocampal formation (Fig. 2*B*,*C*) and the biochemical (Fig. 1*F*) and electrophysiological data (see below) (see Fig. 6) all suggest that this is the case. Altogether, our immunohistochemical analysis suggests that $GABA_{B(1)}$ fails to efficiently localize at distal neuronal sites in the absence of $GABA_{B(2)}$.

Radioligand binding studies in $GABA_{B(2)}^{-/-}$ mice

All known competitive $GABA_B$ ligands bind exclusively to the $GABA_{B(1)}$ subunit (Kaupmann et al., 1998; Kniazeff et al., 2002). We therefore used antagonist radioligand binding to analyze $GABA_{B(1)}$ binding sites in $GABA_{B(2)}^{-/-}$ mice. Saturation binding

experiments at brain membrane preparations with [^{125}I]CGP64213 failed to detect significant numbers of $GABA_{B(1)}$ binding sites in $GABA_{B(2)}^{-/-}$ mice (Fig. 3*A*). The failure to detect antagonist radioligand binding at neuronal membranes from $GABA_{B(2)}^{-/-}$ brains precludes agonist displacement studies. We were therefore unable to determine whether $GABA_B$ agonist affinity is lower in $GABA_{B(2)}^{-/-}$ mice, as one would expect from previous recombinant work showing that $GABA_{B(2)}$ increases agonist affinity at $GABA_{B(1)}$ by ~100-fold (Marshall et al., 1999). More sensitive detection systems, such as [^{125}I]CGP71872 photoaffinity labeling (Fig. 3*B*) and [^{3}H]CGP62349 autoradiography (Fig. 3*C*,*D*), reveal low but significant numbers of $GABA_{B(1)}$ binding sites in $GABA_{B(2)}^{-/-}$ mice. Photoaffinity labeling detects both $GABA_{B(1a)}$ and $GABA_{B(1b)}$ in $GABA_{B(2)}^{-/-}$ tissue (Fig. 3*B*), in agreement with the immunoblot analysis (Fig. 1*E*).

We next used [^{35}S]GTPγS binding to investigate whether the residual $GABA_{B(1)}$ protein in $GABA_{B(2)}^{-/-}$ mice participates in functional receptors (Fig. 4). The [^{35}S]GTPγS binding assay preferentially detects receptors that are coupled to $G\alpha_{i/o}$-type G-proteins, the main effectors of native $GABA_B$ receptors. We did not detect any significant GABA- or baclofen-induced [^{35}S]GTPγS binding in $GABA_{B(2)}^{-/-}$ cortical (Fig. 4) or hippocampal (data not shown) membrane preparations. This indicates that the $GABA_{B(1)}$ protein expressed in $GABA_{B(2)}^{-/-}$ mice is either not coupled to $G\alpha_{i/o}$ or not present in sufficient amounts to generate detectable [^{35}S]GTPγS binding. In $GABA_{B(2)}^{+/-}$ cortical membranes, baclofen and GABA elicit <50% of the [^{35}S]GTPγS binding seen with wild-type membrane preparations (Fig. 4), consistent with the reduced expression levels of $GABA_{B(1)}$ and $GABA_{B(2)}$ proteins (Figs. 1*E*, 3).

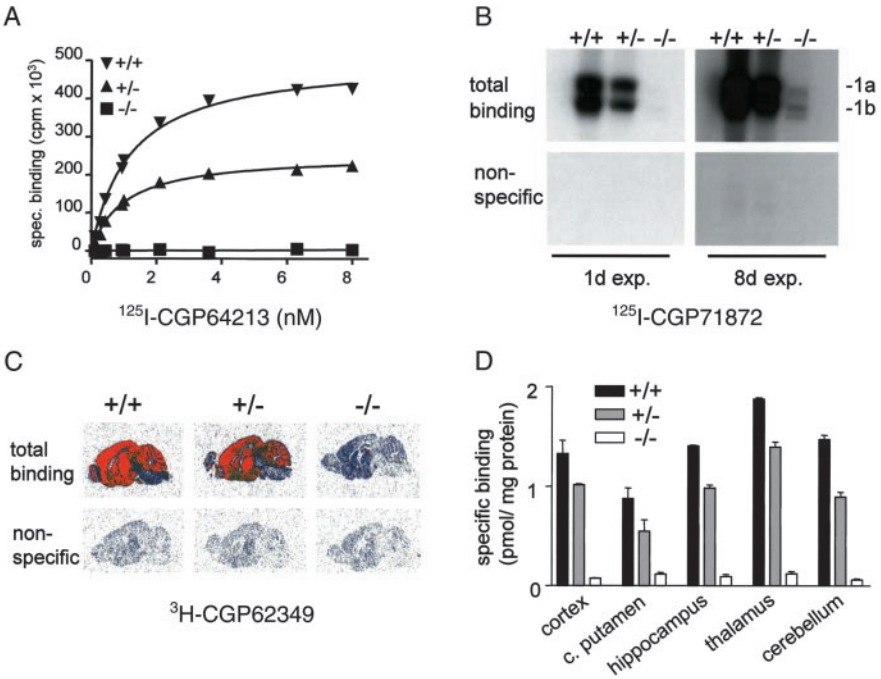

Figure 3. $GABA_{B(1)}$ binding sites in $GABA_{B(2)}^{-/-}$ brains. *A*, Saturation isotherms for [^{125}I]CGP64213 antagonist binding to cortex membranes. No significant binding is detected in membranes from $GABA_{B(2)}^{-/-}$ mice. The number of binding sites is reduced in $GABA_{B(2)}^{+/-}$ versus wild-type mice. The maximal number of binding sites (B_{max}) for wild-type and $GABA_{B(2)}^{+/-}$ mice are 1.4 ± 0.12 and 0.7 ± 0.05 pmol/mg protein, respectively; K_d values were 1.1 ± 0.06 and 0.9 ± 0.05 nM, respectively (mean ± SEM; $n = 3$). *B*, Autoradiograms of brain extracts from wild-type (+/+), $GABA_{B(2)}^{+/-}$ (+/−), and $GABA_{B(2)}^{-/-}$ (−/−) mice, labeled with the photoaffinity antagonist [^{125}I]CGP71872 (0.5 nM) and analyzed by SDS-PAGE. Exposure for 8 d (8d exp.) reveals low amounts of labeled $GABA_{B(1a)}$ (1a) and $GABA_{B(1b)}$ (1b) proteins in $GABA_{B(2)}^{-/-}$ brains. *C*, $GABA_{B(1)}$ subunit autoradiography. Sagittal cryostat sections were incubated with the $GABA_B$ antagonist [^{3}H]CGP62349. Nonspecific binding was determined in the presence of an excess of 100 μM unlabeled L-baclofen. Tritium-sensitive x-ray films were exposed for 24 hr and developed using a Cyclone Storage Phosphor screen (PerkinElmer Life Sciences, Boston, MA). *D*, Quantitative analysis of [^{3}H]CGP62349 receptor autoradiography. Individual brain regions ($n = 3$) were counted using the MCID software package (Imaging Research, St. Catharines, Ontario, Canada). The differences in radioligand binding between the three genotypes are significant (two-sided Dunnett test; $p < 0.001$ for combined analysis of all brain regions). *A–C*, Representative experiments, which were repeated three times.

Loss of presynaptic $GABA_B$ functions in $GABA_{B(2)}^{-/-}$ mice

Electrophysiology provides a more sensitive means than [^{35}S]GTPγS binding for detecting functional $GABA_B$ receptors expressed by individual neurons. We therefore used whole-cell patch-clamp recording to examine $GABA_{B(2)}^{-/-}$ mice for the presence of $GABA_B$ heteroreceptors and autoreceptors on excitatory and inhibitory terminals, respectively. We first studied excitatory synaptic transmission in the hippocampus (Fig. 5*A*,*B*). Stimulation in the Schaffer collateral-commissural fibers induces EPSCs in CA1 pyramidal neurons. The amplitude of these EPSCs is reduced by the activation of $GABA_B$ heteroreceptors or A1 adenosine receptors that inhibit glutamate release (Schuler et al., 2001). Accordingly, in slices from wild-type mice, both baclofen and adenosine evoke the expected depression of the EPSCs (baclofen, 74.0 ± 3.2% inhibition, $n = 4$, $p < 0.01$; adenosine, 85.5 ± 5.3% inhibition, $n = 4$, $p < 0.01$). However, only adenosine has an effect in slices from $GABA_{B(2)}^{-/-}$ mice (baclofen, 0.9 ± 12.6% inhibition, $n = 8$; adenosine, 82.1 ± 7.3% inhibition, $n = 6$, $p < 0.001$). This demonstrates that $GABA_{B(2)}^{-/-}$ mice lack functional $GABA_B$ heteroreceptors on Schaffer collateral terminals, whereas adenosine receptors are still operational and inhibit glutamate release. We next analyzed inhibitory synaptic transmission in the presence of ionotropic glutamate receptor antagonists (Fig. 5*C*,*D*). Activation of $GABA_B$ autoreceptors on interneurons attenuates IPSCs recorded from CA1 pyramidal neurons of wild-type mice (55.3 ± 5.8% inhibition; $n = 7$; $p < 0.001$). In contrast, baclofen is unable to inhibit IPSCs in $GABA_{B(2)}^{-/-}$ mice (−0.5 ± 3.9% inhibition; $n = 6$), although the μ-opioid receptor agonist [D-Ala^2, N-Me-Phe^4, Gly^5-ol]-enkephalin (DAMGO) is still effective in both genotypes (wild-type, 46.5 ± 4.5% inhibition, $n = 7$, $p < 0.001$; $GABA_{B(2)}^{-/-}$ mice, 58.1 ± 3.7% inhibition, $n = 5$, $p < 0.001$). These latter experiments show that hippocampal interneurons lack $GABA_B$ autoreceptors in $GABA_{B(2)}^{-/-}$ mice.

$GABA_B$ receptors inhibit instead of activate K^+ channels in $GABA_{B(2)}^{-/-}$ mice

Postsynaptic $GABA_B$ and adenosine receptors activate a Kir3-mediated K^+ conductance in CA1 pyramidal neurons (Lüscher et al., 1997; Schuler et al., 2001). The $GABA_B$ receptor-activated K^+ conductance underlies the late IPSP (Lüscher et al., 1997). Accordingly, at a holding potential of −50 mV and in physiological $[K^+]_{ext}$, baclofen elicits an outward current in CA1 pyramidal cells of wild-type mice (116.2 ± 26.7 pA; $n = 5$; $p < 0.05$) (Fig.

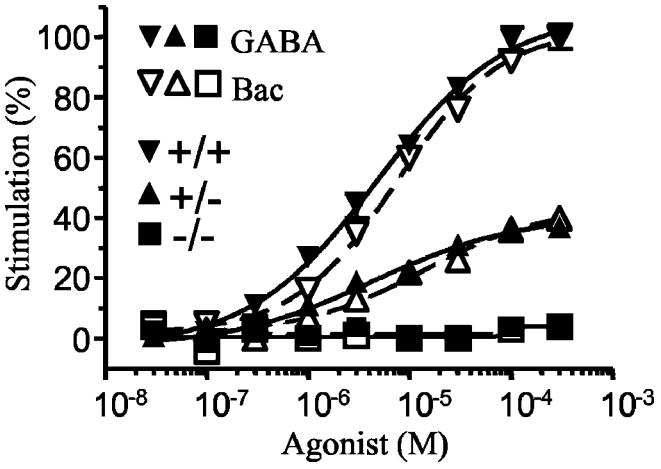

Figure 4. [^{35}S]GTPγS binding to cortex membranes. No significant GABA-stimulated (filled symbols, filled lines) or baclofen-stimulated (Bac; open symbols, dotted lines) [^{35}S]GTPγS binding is detected in $GABA_{B(2)}^{-/-}$ membranes. [^{35}S]GTPγS binding to membranes from $GABA_{B(2)}^{+/-}$ mice is significantly reduced compared with wild-type mice. Values are normalized to the maximal response obtained with wild-type mice.

6*A*,*B*) that is blocked by the $GABA_{B(1)}$ antagonist CGP55845A (2 μM; 93.4 ± 12.5% inhibition; $n = 4$). Surprisingly, but consistent with the strong $GABA_{B(1)}$-IR observed on the soma and proximal dendrites (Fig. 2*B*,*C*), a baclofen-induced current is also seen in CA1 pyramidal neurons of $GABA_{B(2)}^{-/-}$ mice. However, baclofen elicits an inward instead of the typical outward current (−19.2 ± 4.5 pA; $n = 9$; $p < 0.01$) (Fig. 6*A*,*B*). This inward current can be blocked by the $GABA_{B(1)}$ antagonists CGP55845A (2 μM; 99.4 ± 2.7% inhibition; $n = 8$) (Fig. 6*A*) and CGP62349 (4 μM; 87.5 ± 8.3% inhibition; $n = 5$), the ligand that was used for autoradiographic detection of $GABA_{B(1)}$ (Fig. 3*C*). Whereas the baclofen-induced outward current in wild-type mice is associated with a decrease in the input resistance (−93.3 ± 25.8 MΩ; $n = 5$; $p < 0.05$), the inward current in $GABA_{B(2)}^{-/-}$ mice is associated with an increase in input resistance (35.2 ± 12.1 MΩ; $n = 9$; $p < 0.05$). Adenosine-induced currents are similar in wild-type and $GABA_{B(2)}^{-/-}$ mice (wild-type, 67.0 ± 11.1 pA, $n = 5$, $p < 0.01$; $GABA_{B(2)}^{-/-}$, 51.2 ± 3.8 pA, $n = 4$, $p < 0.01$) (Fig. 6*A*,*B*). The current–voltage relationship of baclofen-induced currents reveals a positive slope conductance in wild-type mice (3.0 ± 0.7 nS; $n = 5$; $p < 0.05$) (Fig. 6*C*,*I*), whereas a negative slope conductance is induced in $GABA_{B(2)}^{-/-}$ mice (−2.3 ± 0.5 nS; $n = 10$; $p < 0.01$) (Fig. 6*C*,*I*). Consistent with the baclofen-induced increase in input resistance, a negative slope conductance indicates that baclofen application leads to the closure of ion channels in $GABA_{B(2)}^{-/-}$ mice. The baclofen-induced conductance changes in wild-type and in $GABA_{B(2)}^{-/-}$ mice are completely blocked by the $GABA_{B(1)}$ antagonist CGP55845A (2 μM; wild-type, −0.2 ± 0.4 nS, $n = 4$, $p < 0.05$; $GABA_{B(2)}^{-/-}$, −0.01 ± 0.06 nS, $n = 8$, $p < 0.001$) (Fig. 6*I*). Adenosine-induced conductance changes are similar in wild-type (conductance, 4.83 ± 0.91 nS; $n = 4$; $p < 0.01$; V_{rev}, −94.5 ± 1.2 mV; $n = 4$) and $GABA_{B(2)}^{-/-}$ (4.63 ± 0.83 nS; $n = 4$; $p < 0.01$; V_{rev}, −93.5 ± 2.5 mV; $n = 4$) mice (Fig. 6*D*,*I*). The reversal potential of the baclofen-induced current in $GABA_{B(2)}^{-/-}$ cells is shifted by raising the extracellular [K^+] from 2.7 mM (V_{rev}, −96.7 ± 3.6 mV; $n = 10$; calculated V_{rev} for K^+, −99.5 mV) to 20 mM (V_{rev}, −47.6 ± 7.4 mV; $n = 6$; calculated V_{rev} for K^+, −45.8 mV) (Fig. 6*E*), indicating that a closure of K^+ channels underlies the baclofen-induced conductance change in $GABA_{B(2)}^{-/-}$ neurons. Barium at a concentration of 300 μM completely occludes the baclofen-induced channel closure in wild-type and $GABA_{B(2)}^{-/-}$ CA1 pyramidal cells (data not shown). It is therefore conceivable that the $GABA_B$ receptors in $GABA_{B(2)}^{-/-}$ CA1 neurons and the $GABA_{B(1,2)}$ receptors in wild-type CA1 neurons both couple to Kir3 channels but with opposite effects on channel activity. A large body of *in vitro* data supports that, within the heteromeric $GABA_{B(1,2)}$ receptor, the now-missing $GABA_{B(2)}$ subunit is absolutely necessary for G-protein coupling (Galvez et al., 2001; Margeta-Mitrovic et al., 2001b; Robbins et al., 2001; Duthey et al., 2002; Havlickova et al., 2002). We therefore investigated whether the baclofen-induced closure of K^+ channels in $GABA_{B(2)}^{-/-}$ cells is mediated by G-proteins or not. We recorded postsynaptic responses in the presence of GDPβS, which prevents G-protein activation. Intracellular dialysis of CA1 pyramidal cells from $GABA_{B(2)}^{-/-}$ mice with GDPβS (1 mM for at least 25 min) specifically blocks the induction of postsynaptic currents by baclofen (control, −19.2 ± 4.5 pA, $n = 5$; GDPβS, 0.1 ± 3.9 pA, $n = 5$, $p < 0.01$) (Fig. 6*F*) or adenosine (control, 51.2 ± 3.8 pA, $n = 4$; GDPβS, 2.1 ± 4.9 pA, $n = 5$, $p < 0.05$) (Fig. 6*F*), demonstrating that the baclofen-induced conductance change in $GABA_{B(2)}^{-/-}$ CA1 pyramidal cells is G-protein mediated. It is conceivable that the baclofen-induced inhibition of a K^+ current is the consequence of a dominant-negative effect. For example, $GABA_{B(1)}$ activation in $GABA_{B(2)}^{-/-}$ neurons may sequester G-proteins that are normally associated with other GPCR-activating K^+ channels. Such a baclofen-dependent sequestering of G-proteins would reduce K^+ currents and could underlie the inward current observed in $GABA_{B(2)}^{-/-}$ neurons. We investigated whether baclofen can cross-inhibit the adenosine response by first applying adenosine to CA1 pyramidal cells, followed by a combined application of adenosine and baclofen (Fig. 6*G*,*H*). In both wild-type and $GABA_{B(2)}^{-/-}$ neurons, the effects of adenosine and baclofen are not fully additive, indicating that adenosine and $GABA_B$ receptors share G-proteins and/or effector K^+ channels. However, the cross-inhibitory effect was not larger in $GABA_{B(2)}^{-/-}$ than in wild-type neurons. Although the outcome of these experiments does not completely exclude sequestering, it clearly does not support it. The fact that the baclofen-induced current is blocked by GDPβS also argues against a passive sequestering of G-proteins and shows that activation of G-proteins is necessary to trigger the inward current (Fig. 6*F*). Others and we reported previously a complete loss of postsynaptic baclofen responses in $GABA_{B(1)}^{-/-}$ mice (Prosser et al., 2001; Schuler et al., 2001). We therefore reinvestigated $GABA_{B(1)}^{-/-}$ mice for baclofen-induced responses under identical experimental conditions as used for the analysis of $GABA_{B(2)}^{-/-}$ mice (Fig. 6*I*). Consistent with our previous findings, we do not observe any postsynaptic conductance changes induced by baclofen in $GABA_{B(1)}^{-/-}$ mice. Therefore, exclusively $GABA_{B(2)}^{-/-}$ mice express residual functional $GABA_B$ receptors.

Lack of behavioral responses to baclofen in $GABA_{B(2)}^{-/-}$ mice

In addition to inducing electrophysiological responses, baclofen may also cause detectable behavioral responses in $GABA_{B(2)}^{-/-}$ mice. We therefore studied well known physiological responses to baclofen in $GABA_{B(2)}^{-/-}$ mice. First, we investigated whether baclofen still induces delta waves in the EEG, as shown previously for wild-type mice (Schuler et al., 2001; Kaupmann et al., 2003). Twenty minutes after baclofen application (10 mg/kg, i.p.), delta waves appeared in the EEG of wild-type mice but not in the EEG of $GABA_{B(2)}^{-/-}$ mice (Fig. 7). Ten hours after baclofen administration, the EEG of wild-type mice reverted to normal.

No significant EEG changes were observed in $GABA_{B(2)}^{-/-}$ mice during the entire duration of the experiment. This indicates that the baclofen-induced electrophysiological responses in $GABA_{B(2)}^{-/-}$ mice (Fig. 6) do not result in detectable changes of electrical activity at the network level.

We next investigated whether $GABA_B$ receptors in $GABA_{B(2)}^{-/-}$ mice are able to mediate the well known muscle-relaxant effect of baclofen. Baclofen induces muscle relaxation in wild-type but not in $GABA_{B(2)}^{-/-}$ mice, as shown by the inability or ability, respectively, of the mice to stay on the rotarod during a 5 min period (Fig. 8*A*). Similarly, $GABA_{B(2)}^{-/-}$ mice demonstrate a lack of baclofen-induced hypothermia (Fig. 8*B*). Together, these data indicate that residual $GABA_B$ receptors in $GABA_{B(2)}^{-/-}$ mice are unable to influence muscle relaxation or body temperature.

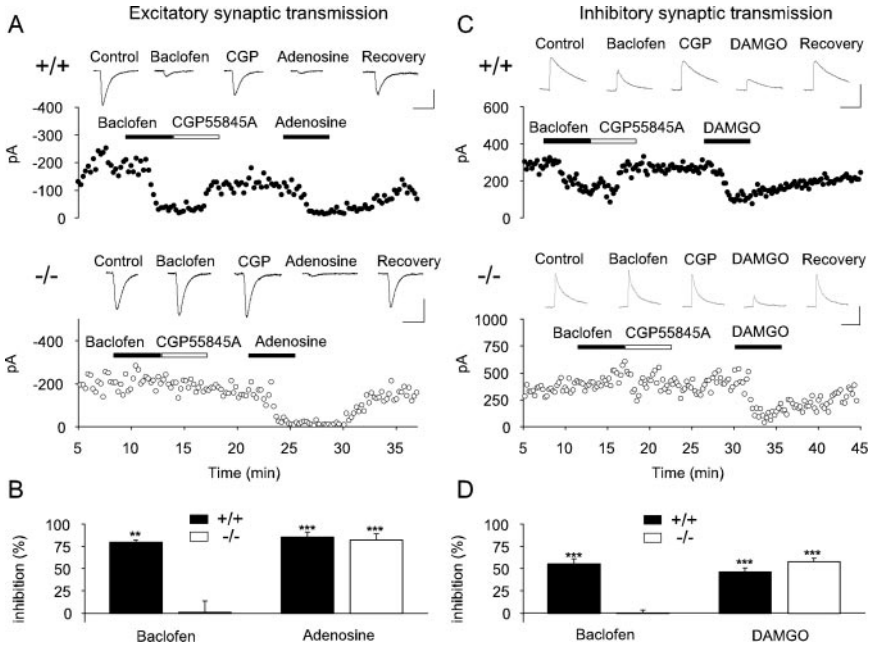

Figure 5. Lack of baclofen-induced presynaptic inhibition in CA1 pyramidal cells of $GABA_{B(2)}^{-/-}$ mice. *A*, Excitatory synaptic transmission. Monosynaptic EPSC peak amplitudes plotted versus time and representative traces from wild-type (top, filled circles) and $GABA_{B(2)}^{-/-}$ (bottom, open circles) mice. Both baclofen (50 μM) and adenosine (100 μM) significantly depress the EPSC amplitude in wild-type mice, whereas baclofen and CGP55845A (2 μM) have no effect on the EPSC amplitude in $GABA_{B(2)}^{-/-}$ mice. The effect of adenosine is similar in both genotypes. Traces are averages of 10 consecutive sweeps. Calibration: 40 msec, 100 pA. *B*, Summary graph showing the lack of baclofen-induced presynaptic inhibition of excitatory synaptic transmission in $GABA_{B(2)}^{-/-}$ mice (wild-type, $n = 4$; $GABA_{B(2)}^{-/-}$, $n = 8$). Adenosine-induced inhibition is similar in both genotypes (wild-type, $n = 4$; $GABA_{B(2)}^{-/-}$, $n = 6$). *C*, Inhibitory synaptic transmission. Monosynaptic IPSC peak amplitudes plotted versus time and representative traces from wild-type (top, filled circles) and $GABA_{B(2)}^{-/-}$ (bottom, open circles) mice. Both baclofen (50 μM) and the μ-opioid agonist DAMGO (1 μM) significantly depress the IPSC amplitude in wild-type mice, whereas baclofen and CGP55845A (2 μM) have no effect on the IPSC amplitude in $GABA_{B(2)}^{-/-}$ mice. The effect of DAMGO was similar in both genotypes. Traces are averages of 10 consecutive sweeps. Calibration: 100 msec, 200 pA. *D*, Summary graph showing the lack of baclofen-induced presynaptic inhibition of inhibitory synaptic transmission in $GABA_{B(2)}^{-/-}$ mice (wild-type, $n = 7$; $GABA_{B(2)}^{-/-}$, $n = 6$). DAMGO-induced inhibition was similar in both genotypes (wild-type, $n = 7$; $GABA_{B(2)}^{-/-}$, $n = 5$). $^{**}p < 0.01$; $^{***}p < 0.001$.

$GABA_{B(2)}^{-/-}$ mice exhibit spontaneous epileptiform activity, hyperlocomotor activity, hyperalgesia, and impaired passive avoidance learning

We reported previously that adult $GABA_{B(1)}^{-/-}$ mice exhibit pronounced spontaneous epileptiform activity (Schuler et al., 2001). We therefore investigated whether adult $GABA_{B(2)}^{-/-}$ mice are epileptic and recorded continuous EEG in freely moving animals using implanted electrodes. $GABA_{B(2)}^{-/-}$ mice displayed several episodes of spontaneous seizures per day. The analysis of three $GABA_{B(2)}^{-/-}$ mice over a 96 hr period revealed an average of 3.75 (0, 11, 3, 1), 0.5 (1, 0, 0, 1), and 2.0 (3, 2, 2, 1) seizures per day. The recorded seizures were exclusively of the clonic type. This is in contrast to $GABA_{B(1)}^{-/-}$ mice, in which additionally absence-type and spontaneous tonic-clonic seizures occurred with low frequency (Schuler et al., 2001). Epileptiform activity was never observed in wild-type littermates ($n = 3$).

$GABA_{B(1)}^{-/-}$ mice exhibit a sporadic hyperlocomotor phenotype when exposed to a new environment (Schuler et al., 2001). We similarly studied the locomotor activity of $GABA_{B(2)}^{-/-}$ mice using the Ethovision recording system. During a 1 hr observation period, $GABA_{B(2)}^{-/-}$ mice moved over a significantly larger distance with significantly increased speed compared with wild-type and heterozygous littermates (Fig. 9*A*). These experiments demonstrate that functional $GABA_B$ receptors in $GABA_{B(2)}^{-/-}$ mice do not rescue the hyperlocomotor phenotype seen with $GABA_{B(1)}^{-/-}$ mice, which completely lack functional $GABA_B$ receptors.

$GABA_B$ agonists exhibit antinociceptive properties in models of acute and chronic pain (Patel et al., 2001). These properties are likely mediated by supraspinal and spinal $GABA_B$ receptors (Malcangio et al., 1991). Consistent with these pharmacological findings, $GABA_{B(1)}^{-/-}$ mice exhibit pronounced hyperalgesia, suggesting that $GABA_B$ receptors exert a tonic control over nociceptive processes (Schuler et al., 2001). We used the hotplate (Fig. 9*B*), tail-flick (Fig. 9*C*), and paw-pressure (Fig. 9*D*) tests to measure acute pain behaviors in $GABA_{B(2)}^{-/-}$ mice. Similar to the $GABA_{B(1)}^{-/-}$ mice, $GABA_{B(2)}^{-/-}$ mice exhibit hyperalgesia in all three tests, showing significantly reduced response latencies or withdrawal thresholds when compared with wild-type or heterozygous littermate mice. In all three tests, we did not observe significant differences in the behavior of wild-type or heterozygous mice.

$GABA_B$ antagonists are reported to have profound effects on memory processing. They can either enhance (Getova and Bowery, 1998; Nakagawa et al., 1999; Stäubli et al., 1999; Getova and Bowery, 2001) or attenuate (Brucato et al., 1996) cognitive performance in a variety of learning paradigms in mice and rats. We reported previously that $GABA_{B(1)}^{-/-}$ mice exhibit a severe impairment of passive avoidance learning (Schuler et al., 2001). We therefore investigated the memory performance of $GABA_{B(2)}^{-/-}$ mice (Fig. 9*E*). $GABA_{B(2)}^{-/-}$ mice, in contrast to wild-type mice, show no increased latency in entering the darkened shock compartment in the retention trial that followed the training trial. This indicates that $GABA_{B(2)}^{-/-}$ mice exhibit an impairment of passive avoidance learning, similar to $GABA_{B(1)}^{-/-}$ mice. We further observed that $GABA_{B(2)}^{-/-}$ mice show increased latencies to enter the darkened shock compartment on the training trial compared with wild-type littermate mice ($p < 0.01$). This excludes the possibility that $GABA_{B(2)}^{-/-}$ mice have a tendency

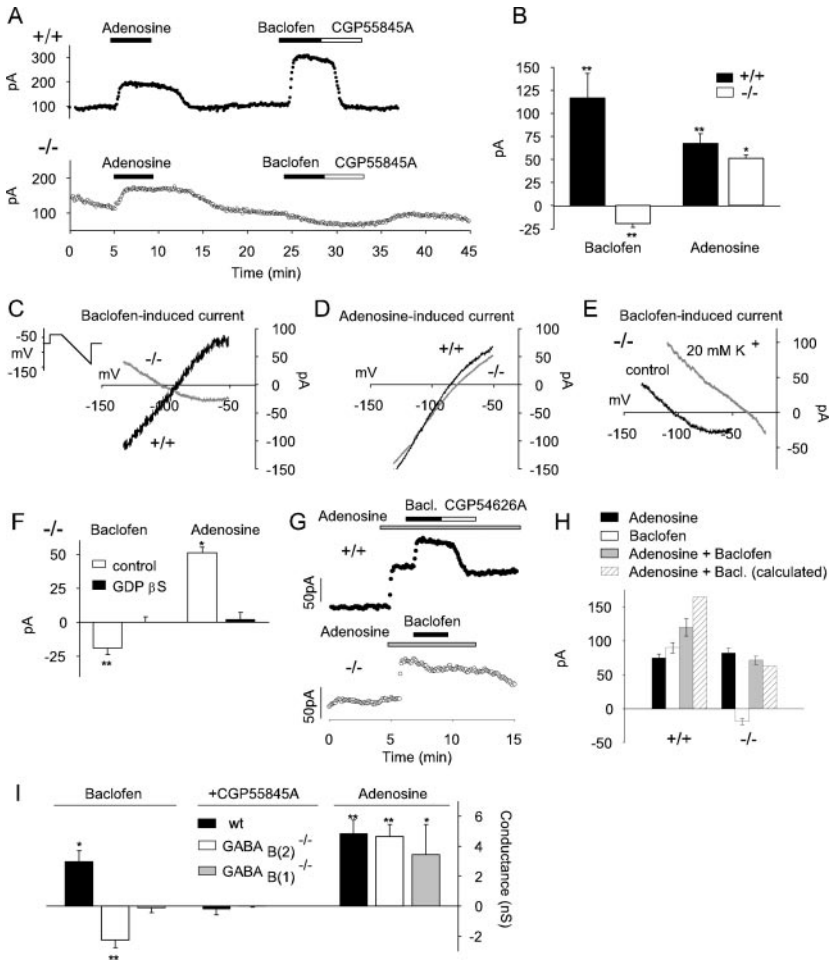

Figure 6. Baclofen inhibits a postsynaptic K^+ conductance in CA1 pyramidal cells of $GABA_{B(2)}^{-/-}$ mice. *A*, Holding current (at −50 mV) plotted versus time for wild-type (top, filled circles) and $GABA_{B(2)}^{-/-}$ (bottom, open circles) mice. Whereas both baclofen (50 μM) and adenosine (100 μM) induce an outward current in wild-type mice, baclofen induces an inward current in $GABA_{B(2)}^{-/-}$ mice. Baclofen-induced effects were blocked by application of the $GABA_B$ receptor antagonist CGP55845A (2 μM) in wild-type as well as in $GABA_{B(2)}^{-/-}$ mice. *B*, Summary graph illustrating the baclofen-induced inward current at −50 mV in $GABA_{B(2)}^{-/-}$ mice. Baclofen-induced currents: wild-type, $n = 5$; $GABA_{B(2)}^{-/-}$, $n = 9$. Adenosine-induced currents: wild-type, $n = 5$; $GABA_{B(2)}^{-/-}$, $n = 4$. *C*, Current–voltage relationship of the baclofen-induced conductance in wild-type (black trace) and $GABA_{B(2)}^{-/-}$ (gray trace) mice. Currents were obtained by calculating the difference between the *I–V* curves before and after addition of baclofen. Whereas a current with a positive slope conductance is induced by baclofen in wild-type mice, a current with negative slope conductance is induced in $GABA_{B(2)}^{-/-}$ mice. *D*, Current–voltage relationship of the adenosine-induced conductance in wild-type mice (black trace) is not different from $GABA_{B(2)}^{-/-}$ mice (gray trace). *E*, Baclofen induces the closure of K^+ channels in $GABA_{B(2)}^{-/-}$ mice. Raising extracellular $[K^+]$ concentration shifts the reversal potential of the baclofen-induced current. *F*, The baclofen-induced conductance change is mediated by G-protein activation. In the presence of intracellular GDPβS (1 mM for 25 min), both the baclofen-induced (control, $n = 5$; GDPβS, $n = 5$) and adenosine-induced (control, $n = 4$; GDPβS, $n = 5$) currents are inhibited in $GABA_{B(2)}^{-/-}$ mice. *G*, Changes in the holding current (at −50 mV) in response to baclofen (Bacl.) after preincubation with adenosine. *H*, Summary graph illustrating that the effects of adenosine and baclofen are not fully additive. In wild-type neurons (+/+), the effect of a combined application of adenosine and baclofen is lower than the sum of the individual effects [Adenosine + Bacl. (calculated)]. In $GABA_{B(2)}^{-/-}$ (−/−) neurons, the effects of adenosine and baclofen are not fully additive. Application of baclofen does not obliterate the adenosine response. *I*, Left, Summary graph illustrating postsynaptic conductance changes induced by baclofen in wild-type ($n = 5$), $GABA_{B(2)}^{+/-}$ ($n = 10$), and $GABA_{B(1)}^{-/-}$ ($n = 4$) mice. The conductance changes were blocked by application of the $GABA_{B(1)}$ receptor antagonist CGP55845A (2 μM; wild-type, $n = 4$; $GABA_{B(2)}^{-/-}$, $n = 8$). Adenosine-induced conductance changes are not different between genotypes (wild-type, $n = 4$; $GABA_{B(2)}^{-/-}$, $n = 4$; $GABA_{B(1)}^{-/-}$, $n = 3$). *$p < 0.05$; **$p < 0.01$.

to enter the dark compartment more quickly, independent of the training experience.

Discussion

Pharmacological and behavioral analyses of $GABA_{B(2)}^{-/-}$ mice indicate that deletion of the $GABA_{B(2)}$ subunit is sufficient to abolish all well known responses to $GABA_B$ agonists, such as $[^{35}S]GTP\gamma S$ binding (Fig. 4), muscle relaxation (Fig. 8*A*), hypothermia (Fig. 8*B*), and EEG delta wave induction (Fig. 7). These findings are paralleled by a loss of typical electrophysiological $GABA_B$ responses in the $GABA_{B(2)}^{-/-}$ hippocampus (Figs. 5, 6). These results are analogous to the results obtained with $GABA_{B(1)}^{-/-}$ mice and suggest that all classical $GABA_B$ responses relate to heteromeric $GABA_{B(1,2)}$ receptors. The heteromeric nature of predominant native $GABA_B$ receptors is further emphasized by the substantial downregulation of $GABA_{B(1)}$ protein in $GABA_{B(2)}^{-/-}$ mice (Fig. 1*E*). An analogous requirement of $GABA_{B(1)}$ for stable expression of $GABA_{B(2)}$ was observed in $GABA_{B(1)}^{-/-}$ mice (Prosser et al., 2001; Schuler et al., 2001; Quéva et al., 2003).

Strikingly, the remaining $GABA_{B(1)}$ protein in $GABA_{B(2)}^{-/-}$ neurons accumulates in distinct cellular compartments than in wild-type neurons. Throughout the $GABA_{B(2)}^{-/-}$ brain, we observed a redistribution of the $GABA_{B(1)}$-IR from the neuropil to the soma (Fig. 2 and data not shown). We also noticed some scattered hippocampal interneurons that are more evident in $GABA_{B(2)}^{-/-}$ than wild-type brains (Fig. 2*B*,*C*). The $GABA_{B(1)}$-IR prominently outlines the soma and proximal dendrites of these cells. This is reminiscent of the strong somatic $GABA_{B(1)}$-IR observed in a subset of GABAergic hippocampal interneurons lacking $GABA_{B(2)}$-IR (Fritschy et al., 1999; Sloviter et al., 1999; Kulik et al., 2003). Presumably, both a genetically induced and a natural lack of $GABA_{B(2)}$ expression leads to a relocation of $GABA_{B(1)}$ protein to the soma and proximal dendrites. Because $GABA_{B(2)}$ is important for exit of $GABA_{B(1)}$ from the ER, most of the somatic $GABA_{B(1)}$-IR likely reflects protein that fails to exit the ER. However, some of the $GABA_{B(1)}$-IR on the soma and proximal dendrites may also represent $GABA_{B(1)}$ protein at the cell surface. This is supported by biochemical (Fig. 1*F*) and electrophysiological (Fig. 6) data that reveal $GABA_{B(1)}$ expression in synaptic membranes and functional receptors in the somatodendritic compartment of CA1 pyramidal neurons, respectively. Besides being important for G-protein coupling and export from the ER (Margeta-Mitrovic et al., 2000, 2001b; Calver et al., 2001; Galvez et al., 2001; Pagano et al., 2001; Robbins et al., 2001), $GABA_{B(2)}$ may therefore also be necessary for the targeting of $GABA_{B(1,2)}$ receptors to the distal zones of neuronal processes.

Whether a physiologically relevant signaling underlies the electrophysiological $GABA_B$ responses that we observe in CA1 neurons of $GABA_{B(2)}^{-/-}$ mice is unclear. It is possible that these $GABA_B$ responses are a consequence of the knock-out situation,

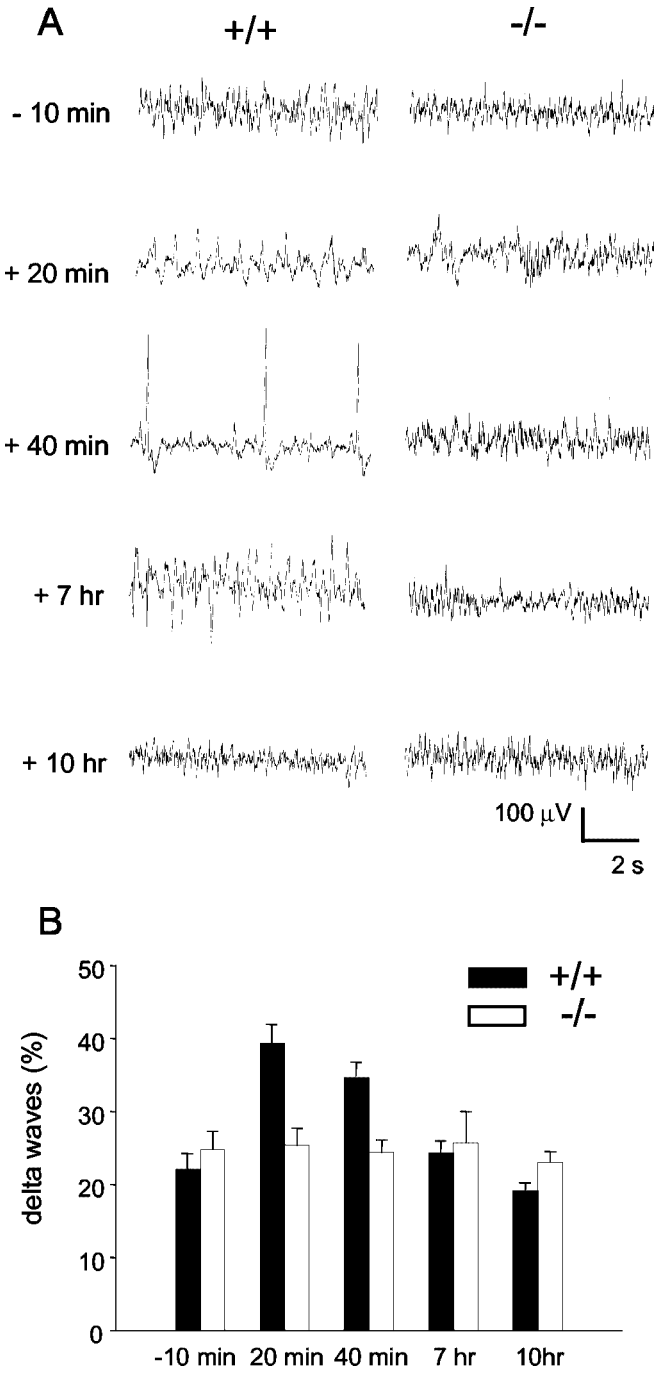

Figure 7. Lack of baclofen-induced delta waves in $GABA_{B(2)}^{-/-}$ mice. *A*, Effect of L-baclofen (10 mg/kg, i.p.) on the EEG of freely moving wild-type (+/+) and $GABA_{B(2)}^{-/-}$ (−/−) mice. The EEG of wild-type and $GABA_{B(2)}^{-/-}$ mice were similar 10 min before baclofen application (−10 min). Twenty minutes after baclofen application, delta waves were observed in the EEG of wild-type, but not of $GABA_{B(2)}^{-/-}$, mice (+20 min). Single spikes appeared sporadically in the EEG of wild-type mice (+40 min), followed by delta waves that lasted for several hours (+7 hr). Ten hours after baclofen application, the EEG traces of wild-type and $GABA_{B(2)}^{-/-}$ mice were again similar (+10 hr). *B*, Quantification of baclofen-induced delta waves in the EEG of wild-type and $GABA_{B(2)}^{-/-}$ mice. The percentage of delta waves of the total power amplitude was calculated over periods of 10 min. Three to four mice per genotype were analyzed.

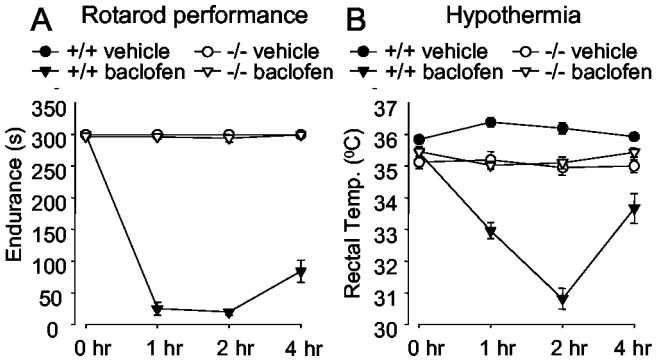

Figure 8. Lack of baclofen-induced motor impairment and hypothermia in $GABA_{B(2)}^{-/-}$ mice. *A*, No baclofen-induced impairment of rotarod endurance is observed in $GABA_{B(2)}^{-/-}$ (−/−) mice ($n = 7$–10). In contrast, wild-type mice (+/+) show a marked reduction in rotarod performance after baclofen application ($p < 0.05$; Fisher's *post hoc* tests). The vehicle-treated control groups stayed on the rotarod during the entire experiment (300 sec) at all time points examined. Thus, in the graph, the data points for the wild-type vehicle control (black dots) are hidden behind the data points for the $GABA_{B(2)}^{-/-}$ vehicle control (white dots). At all time points after baclofen application (1, 2, and 4 hr), the $GABA_{B(2)}^{-/-}$ group (white triangles) differed significantly from the wild-type control group (black triangles) ($p < 0.05$; Fisher's *post hoc* tests). All data points represent mean ± SEM values. *B*, Baclofen induces a potent reduction in body temperature in wild-type mice (black triangles) compared with the vehicle control group (black dots) ($p < 0.05$; Fisher's *post hoc* tests), whereas it is without effect on basal temperature in $GABA_{B(2)}^{-/-}$ mice ($n = 7$–10). However, $GABA_{B(2)}^{-/-}$ mice (white dots) exhibit a slight but significantly reduced basal temperature compared with wild-type littermates (black dots) ($p < 0.05$; Fisher's *post hoc* tests). All data points represent mean ± SEM values.

in which $GABA_{B(1)}$ is expressed in the absence of its usual dimerization partner. An abnormal intracellular accumulation of $GABA_{B(1)}$ protein in $GABA_{B(2)}^{-/-}$ pyramidal cells may overload the ER-retention machinery, thereby allowing some $GABA_{B(1)}$ to escape to the cell surface and to couple to G-proteins. Consistent with this possibility, $GABA_{B(1)}$ was originally expression cloned using [^{125}I]CGP64213 binding on the surface of live COS-1 cells (Kaupmann et al., 1997), showing that some $GABA_{B(1)}$ protein can overcome ER retention in the absence of $GABA_{B(2)}$. In further support of this possibility, no $GABA_B$ responses were detected in CA1 pyramidal neurons of mice expressing a C-terminally truncated version of the $GABA_{B(2)}$ protein (A. Calver, personal communication). Apparently, the truncated $GABA_{B(2)}$ protein dimerizes with $GABA_{B(1)}$ in the ER, generating a dominant-negative situation that impedes transit of $GABA_{B(1)}$ protein through intracellular compartments.

Normally, postsynaptic $GABA_B$ receptors activate a K^+ conductance underlying the late IPSP (Lüscher et al., 1997). However, in $GABA_{B(2)}^{-/-}$ mice, baclofen induces a G-protein-dependent inward current instead of the expected outward current, most likely reflecting the closure of K^+ channels (Fig. 6). Barium at 300 μM occludes the baclofen-induced current inhibition seen in $GABA_{B(2)}^{-/-}$ mice (data not shown). Kir3 channels could therefore not only be the cause of the typical outward current seen in wild-type neurons (Lüscher et al., 1997) but could also be responsible for the atypical inward current seen in $GABA_{B(2)}^{-/-}$ neurons. The $GABA_{B(1)}$ antagonists CGP55845A (Fig. 6*A*,*I*) and CGP62349 (see Results) block the baclofen-induced inward current seen in $GABA_{B(2)}^{-/-}$ CA1 pyramidal cells. A radioactive version of the antagonist used in electrophysiology, [^{3}H]CGP62349, specifically recognizes residual $GABA_{B(1)}$ protein in the $GABA_{B(2)}^{-/-}$ brain (Fig. 3*C*). Moreover, the inward current is not observed in $GABA_{B(1)}^{-/-}$ CA1 pyramidal cells (Fig. 6*I*). Together, this suggests that the baclofen-sensitive current is triggered by receptors incorporating $GABA_{B(1)}$. Baclofen-sensitive currents were seen in the majority of $GABA_{B(2)}^{-/-}$ CA1 neurons analyzed, indicating that the neuronal environment reliably assists functioning of $GABA_{B(1)}$ in the absence of $GABA_{B(2)}$. It remains unclear why the $GABA_{B(1)}$-

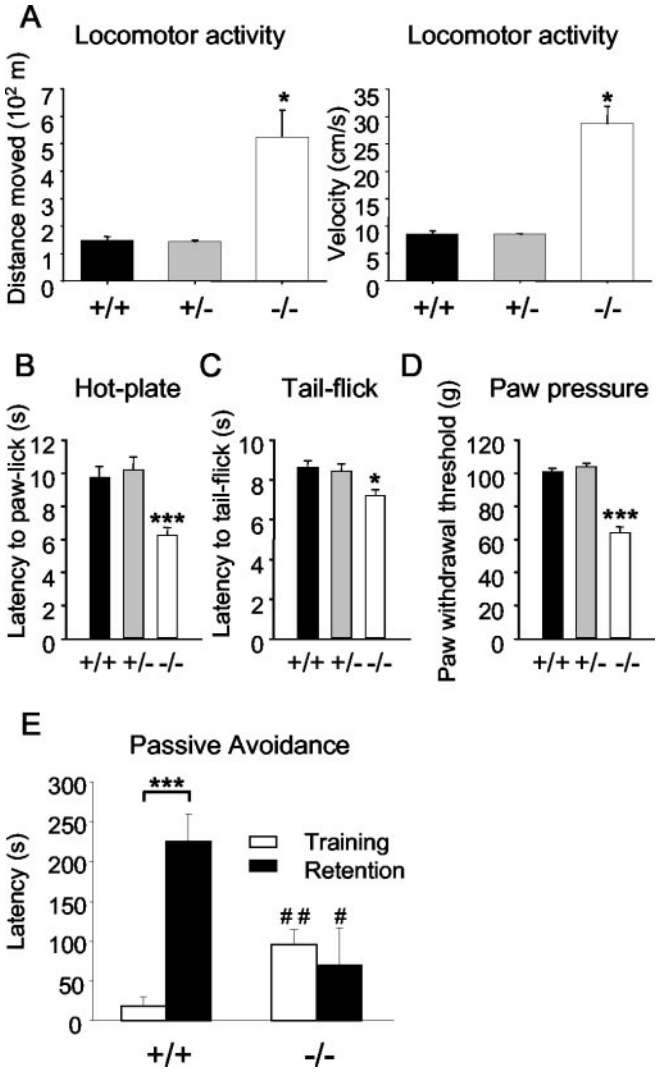

Figure 9. Behavioral analysis of $GABA_{B(2)}^{-/-}$ mice. *A*, Hypolocomotor activity in $GABA_{B(2)}^{-/-}$ mice. During a 1 hr observation period, $GABA_{B(2)}$ knock-out mice (−/−) moved over significantly longer distances (left histogram) with significantly greater speed (right histogram) than heterozygous (+/−) and wild-type (+/+) control mice. $n = 7–8$ per genotype; mean ± SEM; $*p < 0.05$. *B*, Response latencies of wild-type (+/+), heterozygous (+/−), and $GABA_{B(2)}$ knock-out (−/−) mice in the hotplate test assessed at 55°C. $GABA_{B(2)}^{-/-}$ mice show significantly reduced paw-lick latencies compared with wild-type and heterozygous control groups. $n = 19–20$ per genotype; mean ± SEM; $***p < 0.001$. *C*, Response latencies of wild-type (+/+), heterozygous (+/−), and $GABA_{B(2)}$ knock-out (−/−) mice in the tail-flick test assessed at infrared intensity 14. $GABA_{B(2)}^{-/-}$ mice show significantly reduced tail-flick latencies compared with wild-type and heterozygous control groups. $n = 19–21$ per group; mean ± SEM; $*p < 0.05$. *D*, Paw-withdrawal thresholds for wild-type (+/+), heterozygous (+/−), and $GABA_{B(2)}$ knock-out (−/−) mice in response to a mechanical stimulus. Withdrawal thresholds of the left hindpaw were assessed for each genotype. $GABA_{B(2)}^{-/-}$ mice show a significantly reduced withdrawal threshold compared with wild-type and heterozygous control groups. $n = 19–21$ per group; $***p < 0.001$. Nociception tests were analyzed with Tukey's honestly significant difference test. In all tests, there were no significant differences in the behavior of wild-type or heterozygous mice. *E*, Impaired passive avoidance learning in $GABA_{B(2)}^{-/-}$ mice. Step-through latencies of wild-type (+/+) and $GABA_{B(2)}$ knock-out (−/−) mice into the dark (shock) compartment on the training day (white bars) and in the retention test (black bars). $GABA_{B(2)}^{-/-}$ mice were slower to enter on training day but faster in the retention test compared with the wild-type control mice. Wild-type, but not $GABA_{B(2)}^{-/-}$, mice show significantly longer latencies to enter the dark compartment in the retention test compared with the training trial, which is taken as an index of memory of the initial experience. $n = 6–11$ per group; mean ± SEM; $***p < 0.001$ versus training; $\#p < 0.05$ versus genotype; $\#\#p < 0.01$ versus genotype.

mediated electrophysiological responses in $GABA_{B(2)}^{-/-}$ CA1 neurons are opposite to those recorded in wild-type CA1 neurons. We addressed whether activation of $GABA_{B(1)}$ in $GABA_{B(2)}^{-/-}$ neurons takes on a dominant-negative effect by sequestering G-proteins that normally activate Kir channels. We did not observe increased cross-inhibition of the adenosine response by baclofen in $GABA_{B(2)}^{-/-}$ as opposed to wild-type neurons, rendering sequestering unlikely (Fig. 6*G*,*H*). Further arguing against a passive sequestering of G-proteins, the baclofen-induced inward current in $GABA_{B(2)}^{-/-}$ neurons is blocked by GDPβS (Fig. 6*F*). Some G-proteins are reported to inhibit rather than to activate Kir3 channels (e.g., by phospholipase C-mediated phosphatidylinositol-4, 5-biphosphate hydrolysis or PKC activation) (Schreibmayer et al., 1996; Sharon et al., 1997; Lei et al., 2000, 2001; Blanchet and Lüscher, 2002; Mao et al., 2004). Similar to what is now observed, metabotropic glutamate receptors not only activate but also inhibit K^+ channels, presumably by coupling to distinct G-proteins (Sharon et al., 1997). For example, they were shown to be able to suppress a barium-sensitive K^+ current in CA3 pyramidal cells (Lüthi et al., 1997) and to downregulate Kir3 channels in *Xenopus* oocytes (Sharon et al., 1997). It is therefore conceivable that the somatic redistribution of $GABA_B$ receptors (Fig. 2) in $GABA_{B(2)}^{-/-}$ neurons leads to a promiscuous coupling to G-proteins that are not normally associated with heteromeric $GABA_{B(1,2)}$ receptors. This would explain why no significant [^{35}S]GTPγS binding is detectable in neuronal membranes from $GABA_{B(2)}^{-/-}$ mice (Fig. 4) because this assay preferentially detects $G_{i/o}$-proteins that are typically associated with native $GABA_{B(1,2)}$ receptors. A promiscuous coupling to G-proteins in neurons may also explain why we never observed $GABA_B$ responses opposite to those of heteromeric $GABA_{B(1,2)}$ receptors when $GABA_{B(1)}$ was functional by itself in transfected cells (Kaupmann et al., 1997, 1998). There is compelling *in vitro* evidence to show that, in the heteromer, the $GABA_{B(2)}$ subunit is necessary to engage and activate G-proteins (Galvez et al., 2001; Margeta-Mitrovic et al., 2001b; Robbins et al., 2001; Duthey et al., 2002; Havlickova et al., 2002). $GABA_{B(1)}$ may therefore also function in association with another, yet unknown GPCR subunit, which couples to G-proteins other than $GABA_{B(2)}$. In that respect, a $GABA_B$ receptor-related protein has been identified (Calver et al., 2003). However, in heterologous cells, this protein does not appear to participate in typical $GABA_B$ signaling. Furthermore, because "Family C" GPCRs preferentially assemble homodimers, the existence of homodimeric $GABA_{B(1)}$ receptors cannot be excluded (Bouvier, 2001). It is possible that homodimeric $GABA_{B(1)}$ receptors couple to G-proteins other than heterodimeric $GABA_{B(1,2)}$ receptors. Moreover, they may exhibit a constitutive activity that can be inhibited by agonists. Of note, it was reported that chimeric $GABA_B$ receptors with two $GABA_{B(1)}$ extracellular domains exhibit an increased basal activity and, for unknown reasons, respond to GABA agonists with inhibition rather than activation of Kir3 channels (Margeta-Mitrovic et al., 2001a). Similar observations were made in a related study (Galvez et al., 2001).

It is not ruled out that the baclofen-induced inward current is also present in wild-type CA1 pyramidal cells, in which it would be masked by simultaneous larger outward currents activated by heteromeric $GABA_{B(1,2)}$ receptors. Unfortunately, because we lack ligands that distinguish molecular subtypes of $GABA_B$ receptors, genetic manipulation is currently the only means to functionally dissociate native $GABA_B$ assemblies with and without a $GABA_{B(2)}$ subunit. Regardless of whether the baclofen-induced current seen in $GABA_{B(2)}^{-/-}$ CA1 neurons is a consequence of the knock-out situation or not, the observation of a functional $GABA_B$ receptor in the absence of $GABA_{B(2)}^{-/-}$ may be impor-

tant. An increasing number of studies suggest that various cellular populations in the nervous system express $GABA_{B(1)}$ without $GABA_{B(2)}$ (Billinton et al., 2000; Calver et al., 2000; Clark et al., 2000; Ng and Yung, 2001; Burman et al., 2003; Kim et al., 2003; Kulik et al., 2003; Li et al., 2003; Straessle et al., 2003). Our results imply that neurons that naturally lack a $GABA_{B(2)}$ subunit nevertheless have the potential to express functional $GABA_B$ receptors. Unfortunately, it is currently impossible to identify such cells for electrophysiological recordings. This, together with the finding that the $GABA_B$ receptors seen in $GABA_{B(2)}^{-/-}$ mice do not appear to be involved in classical $GABA_B$ functions, makes it currently difficult to address the possible physiological role of such receptors.

In conclusion, it clearly emerges that heteromeric $GABA_{B(1,2)}$ receptors are the prevalent $GABA_B$ receptors in the nervous system and that virtually all $GABA_{B(2)}$ protein is normally associated with $GABA_{B(1)}$. However, our genetic experiments also suggest that $GABA_{B(1)}$ could be functional in neurons that naturally lack $GABA_{B(2)}$ expression.

References

Anderson WW, Collingridge GL (2001) The LTP Program: a data acquisition program for on-line analysis of long-term potentiation and other synaptic events. J Neurosci Methods 108:71–83.

Bettler B, Kaupmann K, Mosbacher J, Gassmann M (2004) Molecular structure and physiological functions of $GABA_B$ receptors. Physiol Rev, in press.

Billinton A, Ige AO, Wise A, White JH, Disney GH, Marshall FH, Waldvogel HJ, Faull RL, Emson PC (2000) $GABA_B$ receptor heterodimer-component localisation in human brain. Brain Res Mol Brain Res 77:111–124.

Blanchet C, Lüscher C (2002) Desensitization of mu-opioid receptor-evoked potassium currents: initiation at the receptor, expression at the effector. Proc Natl Acad Sci USA 99:4674–4679.

Bouvier M (2001) Oligomerization of G-protein-coupled transmitter receptors. Nat Rev Neurosci 2:274–286.

Bowery NG, Bettler B, Froestl W, Gallagher JP, Marshall F, Raiteri M, Bonner TI, Enna SJ (2002) International Union of Pharmacology. XXXIII. Mammalian γ-aminobutyric $acid_B$ receptors: structure and function. Pharmacol Rev 54:247–264.

Brucato FH, Levin ED, Mott DD, Lewis DV, Wilson WA, Swartzwelder HS (1996) Hippocampal long-term potentiation and spatial learning in the rat: effects of $GABA_B$ receptor blockade. Neuroscience 74:331–339.

Burman KJ, Ige AO, White JH, Marshall FH, Pangalos MN, Emson PC, Minson JB, Llewellyn-Smith IJ (2003) $GABA_B$ receptor subunits, R1 and R2, in brainstem catecholamine and serotonin neurons. Brain Res 970:35–46.

Calver AR, Medhurst AD, Robbins MJ, Charles KJ, Evans ML, Harrison DC, Stammers M, Hughes SA, Hervieu G, Couve A, Moss SJ, Middlemiss DN, Pangalos MN (2000) The expression of $GABA_{B(1)}$ and $GABA_{B(2)}$ receptor subunits in the CNS differs from that in peripheral tissues. Neuroscience 100:155–170.

Calver AR, Robbins MJ, Cosio C, Rice SQJ, Babbs AJ, Hirst WD, Boyfield I, Wood MD, Russell RB, Price GW, Couve A, Moss SJ, Pangalos MN (2001) The C-terminal domains of the $GABA_B$ receptor subunits mediate intracellular trafficking but are not required for receptor signaling. J Neurosci 21:1203–1210.

Calver AR, Davies CH, Pangalos MN (2002) $GABA_B$ receptors: from monogamy to promiscuity. Neurosignals 11:299–314.

Calver AR, Michalovich D, Testa TT, Robbins MJ, Jaillard C, Hill J, Szekeres PG, Charles KJ, Jourdain S, Holbrook JD, Boyfield I, Patel N, Medhurst AD, Pangalos MN (2003) Molecular cloning and characterisation of a novel $GABA_B$-related G-protein coupled receptor. Mol Brain Res 110:305–317.

Clark JA, Mezey E, Lam AS, Bonner TI (2000) Distribution of the $GABA_B$ receptor subunit gb2 in rat CNS. Brain Res 860:41–52.

D'Amour FE, Smith DL (1941) A method for determining loss of pain sensation. J Pharmcol Exp Ther 72:74–79.

Duthey B, Caudron S, Perroy J, Bettler B, Fagni L, Pin JP, Prezeau L (2002) A single subunit (GB2) is required for G-protein activation by the heterodimeric $GABA_B$ receptor. J Biol Chem 277:3236–3241.

Eddy NB, Leimbach D (1953) Synthetic analgesics. II. Dithienylbutenyl- and dithienylbutylamines. J Pharmcol Exp Ther 107:385–393.

Filippov AK, Couve A, Pangalos MN, Walsh FS, Brown DA, Moss SJ (2000) Heteromeric assembly of $GABA_B$R1 and $GABA_B$R2 receptor subunits inhibits Ca^{2+} current in sympathetic neurons. J Neurosci 20:2867–2874.

Fritschy JM, Weinmann O, Wenzel A, Benke D (1998) Synapse-specific localization of NMDA and $GABA_A$ receptor subunits revealed by antigen-retrieval immunohistochemistry. J Comp Neurol 390:194–210.

Fritschy JM, Meskenaite V, Weinmann O, Honer M, Benke D, Möhler H (1999) $GABA_B$-receptor splice variants GB1a and GB1b in rat brain: developmental regulation, cellular distribution and extrasynaptic localization. Eur J Neurosci 11:761–768.

Galvez T, Duthey B, Kniazeff J, Blahos J, Rovelli G, Bettler B, Prezeau L, Pin JP (2001) Allosteric interactions between GB1 and GB2 subunits are required for optimal $GABA_B$ receptor function. EMBO J 20:2152–2159.

Getova D, Bowery NG (1998) The modulatory effects of high affinity $GABA_B$ receptor antagonists in an active avoidance learning paradigm in rats. Psychopharmacology (Berl) 137:369–373.

Getova DP, Bowery NG (2001) Effects of high-affinity $GABA_B$ receptor antagonists on active and passive avoidance responding in rodents with gamma-hydroxybutyrolactone-induced absence syndrome. Psychopharmacology (Berl) 157:89–95.

Havlickova M, Prezeau L, Duthey B, Bettler B, Pin JP, Blahos J (2002) The intracellular loops of the GB2 subunit are crucial for G-protein coupling of the heteromeric γ-aminobutyrate B receptor. Mol Pharmacol 62:343–350.

Jones DH, Matus AI (1974) Isolation of synaptic plasma membrane from brain by combined flotation-sedimentation density gradient centrifugation. Biochim Biophys Acta 356:276–287.

Kaupmann K, Huggel K, Heid J, Flor PJ, Bischoff S, Mickel SJ, McMaster G, Angst C, Bittiger H, Froestl W, Bettler B (1997) Expression cloning of $GABA_B$ receptors uncovers similarity to metabotropic glutamate receptors. Nature 386:239–246.

Kaupmann K, Malitschek B, Schuler V, Heid J, Froestl W, Beck P, Mosbacher J, Bischoff S, Kulik A, Shigemoto R, Karschin A, Bettler B (1998) $GABA_B$-receptor subtypes assemble into functional heteromeric complexes. Nature 396:683–687.

Kaupmann K, Cryan JF, Wellendorph P, Mombereau C, Sansig G, Klebs K, Schmutz M, Froestl W, van der Putten H, Mosbacher J, Brauner-Osborne H, Waldmeier P, Bettler B (2003) Specific γ-hydroxybutyrate-binding sites but loss of pharmacological effects of γ-hydroxybutyrate in $GABA_{B(1)}$-deficient mice. Eur J Neurosci 18:2722–2730.

Kim MO, Li S, Park MS, Hornung JP (2003) Early fetal expression of $GABA_{B(1)}$ and $GABA_{B(2)}$ receptor mRNAs on the development of the rat central nervous system. Dev Brain Res 143:47–55.

Kniazeff J, Galvez T, Labesse G, Pin JP (2002) No ligand binding in the GB2 subunit of the $GABA_B$ receptor is required for activation and allosteric interaction between the subunits. J Neurosci 22:7352–7361.

Kulik A, Vida I, Lujan R, Haas CA, Lopez-Bendito G, Shigemoto R, Frotscher M (2003) Subcellular localization of metabotropic $GABA_B$ receptor subunits $GABA_{B(1a/b)}$ and $GABA_{B(2)}$ in the rat hippocampus. J Neurosci 23:11026–11035.

Lei Q, Jones MB, Talley EM, Schrier AD, McIntire WE, Garrison JC, Bayliss DA (2000) Activation and inhibition of G protein-coupled inwardly rectifying potassium (Kir3) channels by G protein $\beta\gamma$ subunits. Proc Natl Acad Sci USA 97:9771–9776.

Lei Q, Talley EM, Bayliss DA (2001) Receptor-mediated inhibition of G protein-coupled inwardly rectifying potassium channels involves Gαq family subunits, phospholipase C, and a readily diffusible messenger. J Biol Chem 276:16720–16730.

Li SP, Park MS, Yoon H, Rhee KH, Bahk JY, Lee JH, Park JS, Kim MO (2003) Differential distribution of $GABA_{B(1)}$ and $GABA_{B(2)}$ receptor mRNAs in the rat brain. Mol Cells 16:40–47.

Lüscher C, Jan LY, Stoffel M, Malenka RC, Nicoll RA (1997) G protein-coupled inwardly rectifying K^+ channels (GIRKs) mediate postsynaptic but not presynaptic transmitter actions in hippocampal neurons. Neuron 19:687–695.

Lüthi A, Gähwiler BH, Gerber U (1997) 1S,3R-ACPD induces a region of negative slope conductance in the steady-state current-voltage relationship of hippocampal pyramidal cells. J Neurophysiol 77:221–228.

Malcangio M, Ghelardini C, Giotti A, Malmberg-Aiello P, Bartolini A (1991) CGP 35348, a new $GABA_B$ antagonist, prevents antinociception and

muscle-relaxant effect induced by baclofen. Br J Pharmacol 103:1303–1308.

Malitschek B, Rüegg D, Heid J, Kaupmann K, Bittiger H, Fröstl W, Bettler B, Kuhn R (1998) Developmental changes in agonist affinity at $GABA_{B(1)}$ receptor variants in rat brain. Mol Cell Neurosci 12:56–64.

Mao J, Wang X, Chen F, Wang R, Rojas A, Shi Y, Piao H, Jiang C (2004) Molecular basis for the inhibition of G protein-coupled inward rectifier K^+ channels by protein kinase C. Proc Natl Acad Sci USA 101:1087–1092.

Margeta-Mitrovic M, Jan YN, Jan LY (2000) A trafficking checkpoint controls $GABA_B$ receptor heterodimerization. Neuron 27:97–106.

Margeta-Mitrovic M, Jan YN, Jan LY (2001a) Ligand-induced signal transduction within heterodimeric $GABA_B$ receptor. Proc Natl Acad Sci USA 98:14643–14648.

Margeta-Mitrovic M, Jan YN, Jan LY (2001b) Function of GB1 and GB2 subunits in G protein coupling of $GABA_B$ receptors. Proc Natl Acad Sci USA 98:14649–14654.

Marshall FH, Jones KA, Kaupmann K, Bettler B (1999) $GABA_B$ receptors—the first 7TM heterodimers. Trends Pharmacol Sci 20:396–399.

Martin SC, Russek SJ, Farb DH (2001) Human $GABA_{B(R)}$ genomic structure: evidence for splice variants in $GABA_{B(R1)}$ but not $GABA_{B(R2)}$. Gene 278:63–79.

Möhler H, Benke D, Fritschy JM (2001) $GABA_B$-receptor isoforms molecular architecture and distribution. Life Sci 68:2297–2300.

Nakagawa Y, Sasaki A, Takashima T (1999) The $GABA_B$ receptor antagonist CGP36742 improves learned helplessness in rats. Eur J Pharmacol 381:1–7.

Ng TKY, Yung KKL (2001) Differential expression of $GABA_{B(1)}$ and $GABA_{B(2)}$ receptor immunoreactivity in neurochemically identified neurons of the rat neostriatum. J Comp Neurol 433:458–470.

Olpe HR, Karlsson G, Pozza MF, Brugger F, Steinmann M, Van Riezen H, Fagg G, Hall RG, Froestl W, Bittiger H (1990) CGP 35348: a centrally active blocker of $GABA_B$ receptors. Eur J Pharmacol 187:27–38.

Pagano A, Rovelli G, Mosbacher J, Lohmann T, Duthey B, Stauffer D, Ristig D, Schuler V, Meigel I, Lampert C, Stein T, Prezeau L, Blahos J, Pin JP, Froestl W, Kuhn R, Heid J, Kaupmann K, Bettler B (2001) C-terminal interaction is essential for surface trafficking but not for heteromeric assembly of $GABA_B$ receptors. J Neurosci 21:1189–1202.

Patel S, Naeem S, Kesingland A, Froestl W, Capogna M, Urban L, Fox A (2001) The effects of $GABA_B$ agonists and gabapentin on mechanical hyperalgesia in models of neuropathic and inflammatory pain in the rat. Pain 90:217–226.

Prosser HM, Gill CH, Hirst WD, Grau E, Robbins M, Calver A, Soffin EM, Farmer CE, Lanneau C, Gray J, Schenck E, Warmerdam BS, Clapham C, Reavill C, Rogers DC, Stean T, Upton N, Humphreys K, Randall A, Geppert M, Davies CH, Pangalos MN (2001) Epileptogenesis and enhanced prepulse inhibition in $GABA_{B(1)}$-deficient mice. Mol Cell Neurosci 17:1059–1070.

Quéva C, Bremner-Danielsen M, Edlund A, Ekstrand AJ, Elg S, Erickson S, Johansson T, Lehmann A, Mattsson JP (2003) Effects of GABA agonists on body temperature regulation in $GABA_{B(1)}^{-/-}$ mice. Br J Pharmacol 140:315–322.

Randall LO, Selitto JJ (1957) A method for measurement of analgesic activity on inflamed tissue. Arch Int Pharmacodyn Ther 4:409–419.

Robbins MJ, Calver AR, Filippov AK, Hirst WD, Russell RB, Wood MD, Nasir S, Couve A, Brown DA, Moss SJ, Pangalos MN (2001) $GABA_{B(2)}$ is essential for G-protein coupling of the $GABA_B$ receptor heterodimer. J Neurosci 21:8043–8052.

Schreibmayer W, Dessauer CW, Vorobiov D, Gilman AG, Lester HA, Davidson N, Dascal N (1996) Inhibition of an inwardly rectifying K^+ channel by G-protein α-subunits. Nature 380:624–627.

Schuler V, Lüscher C, Blanchet C, Klix N, Sansig G, Klebs K, Schmutz M, Heid J, Gentry C, Urban L, Fox A, Spooren W, Jaton AL, Vigouret JM, Pozza M, Kelly PH, Mosbacher J, Froestl W, Käslin E, Korn R, Bischoff S, Kaupmann K, van der Putten H, Bettler B (2001) Epilepsy, hyperalgesia, impaired memory, and loss of pre- and postsynaptic $GABA_B$ responses in mice lacking $GABA_{B(1)}$. Neuron 31:47–58.

Sharon D, Vorobiov D, Dascal N (1997) Positive and negative coupling of the metabotropic glutamate receptors to a G protein-activated K^+ channel, GIRK, in *Xenopus* oocytes. J Gen Physiol 109:477–490.

Sloviter RS, Ali-Akbarian L, Elliott RC, Bowery BJ, Bowery NG (1999) Localization of $GABA_{B(R1)}$ receptors in the rat hippocampus by immunocytochemistry and high resolution autoradiography, with specific reference to its localization in identified hippocampal interneuron subpopulations. Neuropharmacology 38:1707–1721.

Stäubli U, Scafidi J, Chun D (1999) $GABA_B$ receptor antagonism: facilitatory effects on memory parallel those on LTP induced by TBS but not HFS. J Neurosci 19:4609–4615.

Straessle A, Loup F, Arabadzisz D, Ohning GV, Fritschy JM (2003) Rapid and long-term alterations of hippocampal $GABA_B$ receptors in a mouse model of temporal lobe epilepsy. Eur J Neurosci 18:2213–2226.

Urwyler S, Mosbacher J, Lingenhoehl K, Heid J, Hofstetter K, Froestl W, Bettler B, Kaupmann K (2001) Positive allosteric modulation of native and recombinant γ-aminobutyric $acid_B$ receptors by 2,6-Di-tert-butyl-4-(3-hydroxy-2,2-dimethyl-propyl)-phenol (CGP7930) and its aldehyde analog CGP13501. Mol Pharmacol 60:963–971.

Venable N, Kelly PH (1990) Effects of NMDA receptor antagonists on passive avoidance learning and retrieval in rats and mice. Psychopharmacology (Berl) 100:215–221.